Transport pathways for Asian pollution outflow over the Pacific: Interannual and seasonal variations

Hongyu Liu,[1] Daniel J. Jacob, Isabelle Bey,[2] Robert M. Yantosca, and Bryan N. Duncan[2]
Department of Earth and Planetary Sciences and Division of Engineering and Applied Sciences, Harvard University, Cambridge, Massachusetts, USA

Glen W. Sachse
NASA Langley Research Center, Hampton, Virginia, USA

Received 30 October 2002; revised 21 March 2003; accepted 29 April 2003; published 20 September 2003.

[1] The meteorological pathways contributing to Asian pollution outflow over the Pacific are examined with a global three-dimensional model analysis of CO observations from the Transport and Chemical Evolution over the Pacific (TRACE-P) aircraft mission (February–April 2001). The model is used also to place the TRACE-P observations in an interannual (1994–2001) and seasonal context. The major process driving Asian pollution outflow in spring is frontal lifting ahead of southeastward-moving cold fronts (the leading edge of cold surges) and transport in the boundary layer behind the cold fronts. Orographic lifting over central and eastern China combines with the cold fronts to promote the transport of Chinese pollution to the free troposphere. Outflow of seasonal biomass burning in Southeast Asia during spring takes place mostly by deep convection but also by northeastward transport and frontal lifting, mixing with the anthropogenic outflow. Boundary layer outflow over the western Pacific is largely devoid of biomass burning influence. European and African (biomass burning) plumes in Asian outflow during TRACE-P were weak (<60 ppbv and 20 ppbv CO, respectively) and were not detectable in the observations because of superposition of the much larger Asian pollution signal. Spring 2001 (La Niña) was characterized by unusually frequent cold surge events in the Asian Pacific rim and strong convection in Southeast Asia, leading to unusually strong boundary layer outflow of anthropogenic emissions and convective outflow of biomass burning emissions in the upper troposphere. The Asian outflow flux of CO to the Pacific is found to vary seasonally by a factor of 3–4 (maximum in March and minimum in summer). The March maximum results from frequent cold surge events and seasonal biomass burning emissions. *INDEX TERMS:* 0368 Atmospheric Composition and Structure: Troposphere—constituent transport and chemistry; 0365 Atmospheric Composition and Structure: Troposphere—composition and chemistry; 3364 Meteorology and Atmospheric Dynamics: Synoptic-scale meteorology; *KEYWORDS:* pollution transport, outflow pathways, carbon monoxide, biomass burning, interannual variability

Citation: Liu, H., D. J. Jacob, I. Bey, R. M. Yantosca, B. N. Duncan, and G. W. Sachse, Transport pathways for Asian pollution outflow over the Pacific: Interannual and seasonal variations, *J. Geophys. Res.*, *108*(D20), 8786, doi:10.1029/2002JD003102, 2003.

1. Introduction

[2] Rapid industrialization is taking place over the Asian continent, and energy consumption in Asia is expected to continue to increase in the next few decades. Atmospheric observations of Asian outflow downwind of the continent can be used to test and improve our understanding of Asian emissions and of the export of Asian pollution to the global atmosphere. This was one of the major objectives of the NASA Transport and Chemical Evolution over the Pacific (TRACE-P) aircraft mission conducted over the western Pacific during February–April 2001 [*Jacob et al.*, 2003]. Proper interpretation of Asian outflow observations in terms of Asian emissions and export requires an understanding of outflow pathways and their variability on synoptic, seasonal, and interannual scales. We address here this issue with a global three-dimensional (3-D) chemical tracer model (GEOS-CHEM CTM) [*Bey et al.*, 2001a] driven by assimilated meteorological observations. The model is used to examine the different features of Asian outflow observed during TRACE-P and to place the TRACE-P data in a seasonal and interannual context.

[3] Transport of pollution from continental source regions takes place either within the boundary layer (BL) or in the

[1]Now at National Institute of Aerospace, Hampton, Virginia, USA.
[2]Now at Ecole Polytechnique Federale de Lausanne, Lausanne, Switzerland.

0148-0227/03/2002JD003102$09.00

free troposphere (FT). Transport in the FT is usually faster because of stronger winds. Transport of pollution from the BL to FT takes place by fronts, convection, and orographic forcing. Convection has long been recognized as an effective mechanism for the transport of surface pollutants to the FT [e.g., *Dickerson et al.*, 1987; *Pickering et al.*, 1992]. The role of fronts has received less attention. *Brown et al.* [1984] and *Banic et al.* [1986] were among the first who recognized frontal systems as an important mechanism in the vertical redistribution of pollutants. Both aircraft observations of trace gases in fronts [e.g., *Bethan et al.*, 1998] and modeling studies [*Stohl*, 2001; *Donnell et al.*, 2001; *Kowol-Santen et al.*, 2001; *Bey et al.*, 2001b] have shown clear evidence of frontal lifting of pollutants from the BL to FT. Such frontal lifting largely explains the vertical transport of the BL pollution to the FT in the main ascending branch of an extratropical cyclone (the warm conveyor belt (WCB)) [*Stohl*, 2001; *Cooper et al.*, 2001]. The role of orographically forced vertical advection in pollutant transport was noted by *Donnell et al.* [2001] over the Alps. In addition, turbulent mixing may transport pollutants out of the BL either by detrainment or due to the collapse of the BL [*Donnell et al.*, 2001].

[4] Several previous studies have examined the mechanisms for outflow of Asian pollution to the Pacific. *Carmichael et al.* [1998] found that continental outflow of precursors occurring behind cold fronts has a strong influence on surface ozone levels over Japan during spring. *Yienger et al.* [2000] showed that the development of low-pressure baroclinic systems over Asia, which vent the BL and lift pollution into the FT, is an important mechanism for the episodic export of pollution from Asia. *Bey et al.* [2001b] examined Asian outflow over the western Pacific during the NASA Pacific Exploratory Mission-West B (PEM-West B) aircraft mission (February–March, 1994). They found that frontal lifting of pollution over central and eastern China ahead of eastward moving cold fronts, followed by westerly transport in the lower FT, was the principal process responsible for export of both anthropogenic and biomass burning pollution from Asia. They further found that effluents from seasonal biomass burning in Southeast Asia were mixed with anthropogenic pollution in the FT frontal outflow, and that the BL outflow was mainly anthropogenic and confined to north of 35°N.

[5] Asian outflow of pollution to the Pacific also includes contributions from intercontinental transport. Using trajectory calculations, *Newell and Evans* [2000] emphasized the important influence of European pollution on the Asian outflow in winter. *Bey et al.* [2001b] found that European anthropogenic sources and African biomass burning make major contributions to the Asian outflow of CO in spring; the former dominates the Asian outflow in the BL north of 40°N, and the latter is important in the upper troposphere (UT) at low latitudes. *Liu et al.* [2002] showed that European and North American anthropogenic sources as well as African biomass burning emissions contribute significantly to tropospheric ozone over the Asian Pacific rim.

[6] The TRACE-P aircraft mission used two aircraft (DC-8 and P-3B) to sample a range of Asian outflow patterns, including frontal outflow, postfrontal BL outflow, and convective outflow in the UT [*Jacob et al.*, 2003]. A meteorological overview of the TRACE-P period is given by *Fuelberg et al.* [2003]. In the present study we use CO as a tracer to diagnose the major outflow pathways and transport mechanisms for export of Asian anthropogenic and biomass burning pollution and the pathways for intercontinental transport of pollution contributing to Asian outflow in spring. CO is an excellent tracer for long-range pollution transport [*Staudt et al.*, 2001; *Bey et al.*, 2001b] because (1) it is a general product of incomplete combustion, with major sources from vehicles, biofuels, and biomass burning [*Streets et al.*, 2003], (2) it has a lifetime of a few months, sufficiently long to track pollution plumes on synoptic and intercontinental scales, but sufficiently short to provide strong pollution enhancements in these plumes relative to background, and (3) it can be measured with high precision and temporal resolution. During TRACE-P, spectroscopic measurements of CO were taken using the Differential Absorption CO Measurement (DACOM) with a sampling frequency of 1 Hz and an estimated precision of 2% [*Sachse et al.*, 1987]. We use in this study the 1-min merged data set prepared at NASA Langley Research Center. Our GEOS-CHEM simulation of CO for the TRACE-P period focuses on interpreting and generalizing the aircraft observations. We also present simulations for different seasons and different years (including different phases of El Niño-Southern Oscillation (ENSO)) to place the TRACE-P results in an interannual and seasonal context.

2. Model Description

[7] Global GEOS-CHEM simulations of CO were conducted for the springs (1 February 1–15 April) of 1994, 1998, 2000, and 2001, and for the full year of 1996. The simulation years were chosen so as to cover the TRACE-P (2001) and PEM-West B (1994) missions, as well as different phases of ENSO. The GEOS-CHEM model is driven by assimilated meteorological observations with 3- to 6-hour resolution from the Goddard Earth Observing System (GEOS) of the NASA Data Assimilation Office (DAO). A basic description of the model was given by *Bey et al.* [2001a]. We use here GEOS-CHEM version 4.13 (see http://www-as.harvard.edu/chemistry/trop/geos). The simulations are initialized on 1 January of each year using results from a 2-year simulation driven by 1996 meteorological data. This initialization serves the purpose of providing a realistic CO background.

[8] The simulation of transport in the GEOS-CHEM model uses archived GEOS data for winds, mixing depths, and convective mass fluxes. Three generations of GEOS meteorological products are used for the simulation years as follows: GEOS1 for 1994 ($2° \times 2.5°$ horizontal resolution, 20 vertical levels), GEOS1-STRAT for 1996 ($2° \times 2.5°$, 46 levels), and GEOS3 for 1998, 2000 and 2001 ($1° \times 1°$, 48 levels). The vertical levels are defined along a sigma coordinate. The midpoints of the lowest four levels in the GEOS1 and GEOS1-STRAT data are at 50, 250, 600, and 1100 m above the surface for a column based at sea level. The GEOS3 data have finer resolution of the BL with layer midpoints at 10, 50, 100, 200, 350, 600, 850, and 1250 m above the surface. Further details on the vertical grids are in the work of *Bey et al.* [2001a]. GEOS-CHEM simulations

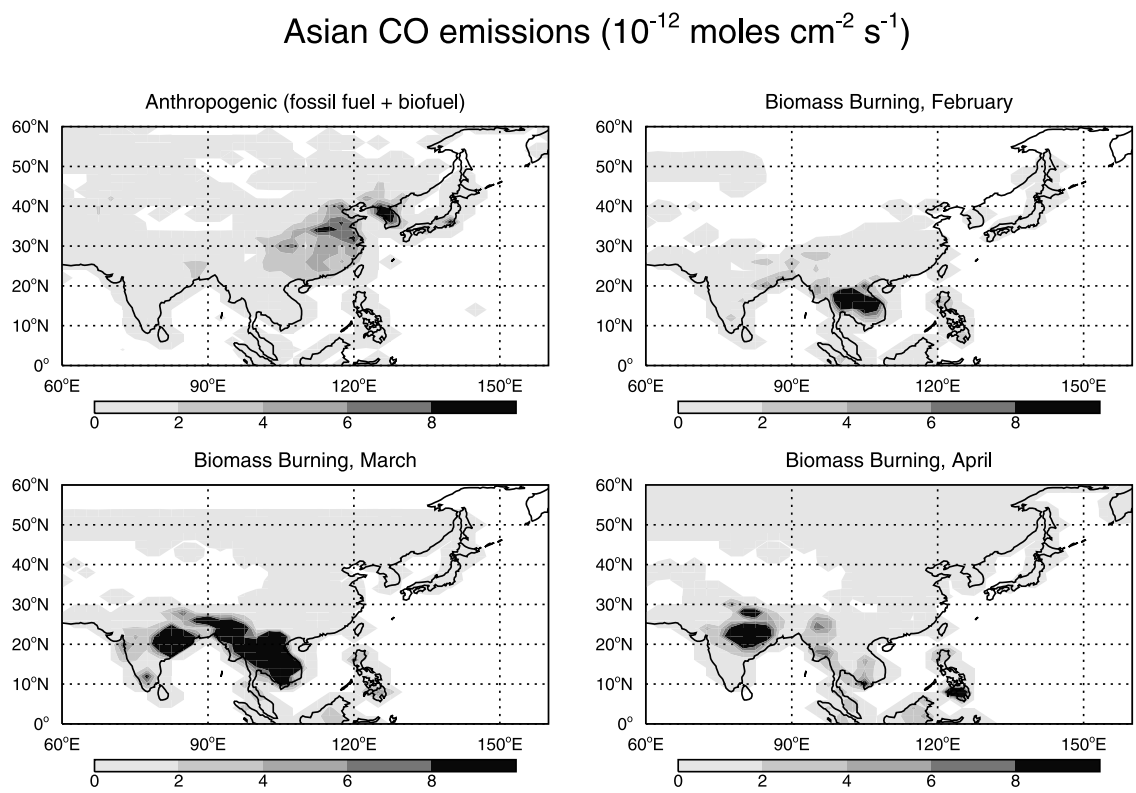

Figure 1. Asian CO emissions (10^{-12} moles cm^{-2} s^{-1}) used in the model for all simulation years. See color version of this figure at back of this issue.

are done with 2° × 2.5° resolution for 1994, 1998, 2000, and 2001 and 4° × 5° for 1996.

[9] The model uses the advection scheme of *Lin and Rood* [1996] with a flux form semi-Lagrangian method, and the moist convective mixing scheme of *Allen et al.* [1996] applied to the GEOS convective updraft, entrainment, and detrainment mass fluxes from the relaxed Arakawa-Schubert algorithm [*Arakawa and Schubert*, 1974; *Moorthi and Suarez*, 1992]. We assume rapid vertical mixing within the GEOS-diagnosed mixed layer driven by surface instability [*Takacs et al.*, 1994].

[10] A detailed description and global evaluation of the GEOS-CHEM simulation for CO is presented by B. N. Duncan et al. (Model study of the variability and trends of carbon monoxide (1988–1997): 1. Model formulation, evaluation, and sensitivity, submitted to *Journal of Geophysical Research*, 2003, hereinafter referred to as Duncan et al., submitted manuscript, 2003). We conduct here a CO-only simulation using archived OH fields from a full chemistry simulation, as was done previously by *Bey et al.* [2001b]. CO sources in the model include anthropogenic emissions (fossil fuel and biofuel), biomass burning emissions and chemical production from oxidation of methane, isoprene, and other volatile organic compounds (VOCs). *Bey et al.* [2001b] previously showed that the model reproduces well the latitudinal and vertical gradients of CO observed over the western Pacific during the PEM-West B period. The low CO (and high OH) in this earlier version of the model has been improved in the current version by the consideration of minor sources from oxidation of previously neglected VOCs (Duncan et al., submitted manuscript, 2003).

[11] We use here aseasonal 1994 anthropogenic emissions from Duncan et al. (submitted manuscript, 2003) (Figure 1) for all simulation years (1994, 1998, 2000, and 2001) in order to focus on variability in transport. The 1994 anthropogenic emission for Asia (0°–60°N, 65°–150°E) is 270.6 Tg yr^{-1} for CO. Biomass burning emissions are from a climatology by *Duncan et al.* [2003] (Figure 1), where the spatial and seasonal variability are derived from satellite observations of monthly total fire counts. Biomass burning over Southeast Asia takes place during December–May and peaks in March, while biomass burning over northern Africa takes place during December–March. GEOS-CHEM simulations of CO for the TRACE-P period indicate that the Duncan et al. (submitted manuscript, 2003) anthropogenic emissions are consistent with TRACE-P and concurrent satellite (MOPITT) CO observations but that the biomass burning emissions are 50–70% too high [*Heald et al.*, 2003; *Palmer et al.*, 2003]. Bias in the biomass burning emissions would affect the relative contributions of biomass burning versus anthropogenic emissions in the simulations presented below.

[12] The major sink of CO is reaction with OH. We use monthly mean OH concentrations generated with a standard full chemistry simulation to calculate loss of CO and production of CO from oxidation of hydrocarbons. Neglect of diurnal and day-to-day variability of OH has a minor effect on our simulated CO concentrations, because of the relatively long lifetime of CO and the fact that loss of CO by OH is partly compensated by CO production from hydrocarbons. Stratospheric OH concentration fields are monthly means provided by the 2-D model of *Schneider et al.* [2000]. Dry deposition of CO is neglected in the model.

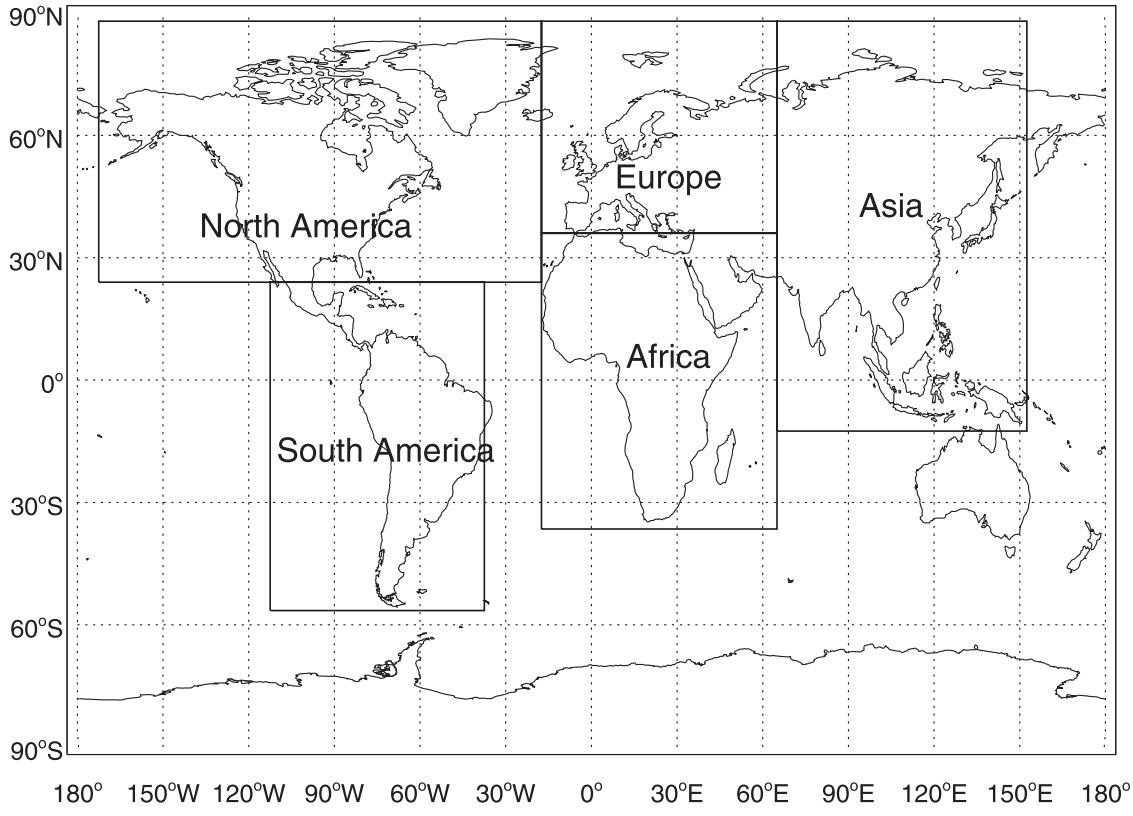

Figure 2. Source regions for tagged CO tracer simulations.

[13] To identify source regions and types contributing to the Asian outflow, we transport separately in the model a suite of CO tracers, all removed with the same loss frequency (OH concentrations) as the total CO. There are four tracers for anthropogenic emissions (Asia, Europe, North America, and the rest of the world) and four tracers for biomass burning (Asia, Africa, South America, and the rest of the world) (Figure 2). Since our simulation of CO is linear, the sum of the separate tracers is close to the total simulated CO concentrations [*Bey et al.*, 2001b].

3. Pathways for Asian Outflow

[14] Figure 3 shows the simulated latitude-altitude cross section at 140°E of monthly mean concentrations and eastward fluxes of Asian CO for March 2001 (TRACE-P). Asian pollution outflow is strongest at 30°–45°N in the BL and at 20°–35°N in the lower FT. The tagged tracer simulation shows that the former mostly reflects anthropogenic emissions and the latter includes contributions from both anthropogenic and biomass-burning emissions (not shown). The UT outflow largely reflects biomass-burning emissions in Southeast Asia lifted by convection. We thus see illustrated the three main pathways for Asian pollution outflow to the Pacific in spring [*Bey et al.*, 2001b]: (1) large-scale lifting by southeastward moving cold fronts and orographic features followed by eastward transport in the lower FT, (2) transport in the BL behind the cold fronts, and (3) convective transport. Here we select some CO outflow episodes observed in TRACE-P, and the corresponding GEOS-CHEM simulation, to illustrate each of these transport pathways as well as contributions from intercontinental transport to Asian outflow. Since CO sources and sinks in the model are not tailored for the TRACE-P period, the focus of model comparison with observations is on plume structures rather than absolute concentrations.

3.1. Frontal Outflow and Postfrontal Boundary Layer Outflow

[15] An important feature of the East Asian winter monsoon is episodic incursion of cold midlatitude air and its penetration deep into the South China Sea [*Boyle and Chen*, 1987; *Slingo*, 1998; *Compo et al.*, 1999]. These so-called "cold surges" are triggered by the extension of the Siberian anticyclone southeastward over China in association with the passage of midlatitude synoptic waves [*Ding*, 1990]. They are confined to the lower troposphere (below 700 hPa) and recur with a frequency of 2–7 days. Cold surges tend to enhance subtropical and tropical deep convection because of the intense low-level convergence along their leading edge [*Garreaud*, 2001]. As the surges move into low latitudes (as far south as 17°N), their characteristics may be lost due to strong surface heat fluxes. This frontal activity is most frequent in spring (peaking in March) and fall (peaking in November) [*Zhang et al.*, 1997].

[16] Various definitions of the cold surges are found in the literature [*Boyle and Chen*, 1987]. Instead of using more rigorous criteria, we simply define the passage of a cold front as the occurrence of an increase in surface pressure and a decrease in surface temperature in central eastern China. Figure 4 shows the time evolution of surface temperature at (30°N, 115°E) during the period

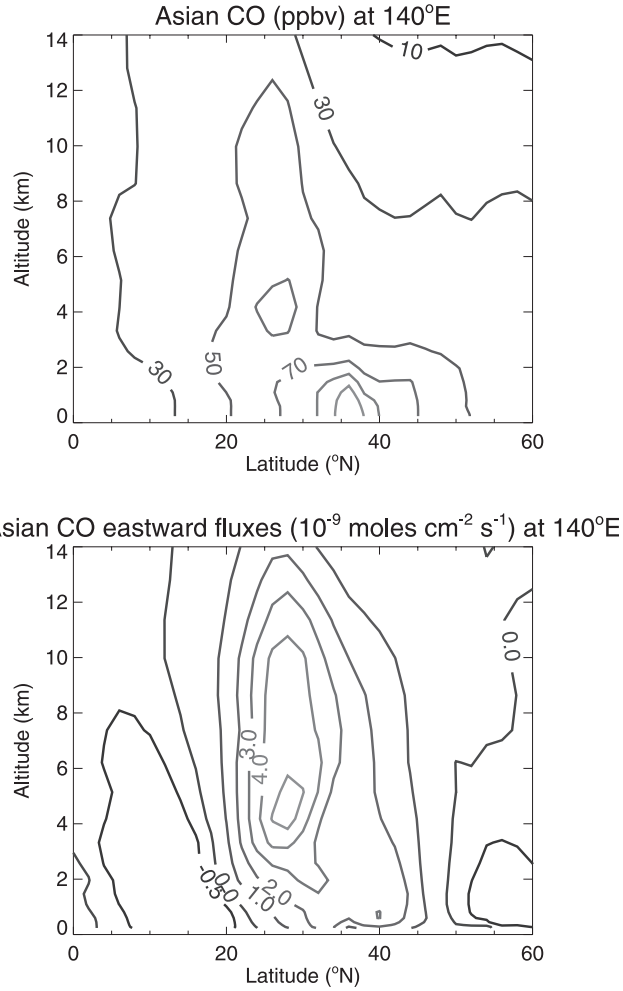

Figure 3. Latitude-altitude cross sections at 140°E of monthly mean concentrations (ppbv, top panel) and fluxes (10^{-12} moles cm^{-2} s^{-1}, bottom panel) of the Asian CO tracer for March 2001. Contour levels are 10, 30, 50, 70, 90, and 110 for concentrations and −0.5, 0, 1, 2, 3, 4, and 5 for fluxes.

of 1 February–15 April 2001. Cold surges are manifested by rapid increase in surface pressure (not shown) and decrease in surface temperature along the East Asian coast. A total of ∼10 surges occurred (i.e., with a period of ∼7 days) during this period. A vigorous cold surge occurred on 6 March during TRACE-P deployment in Hong Kong, when surface air temperature dropped and mean sea level pressure increased rapidly over South China. On 7 March, its leading edge produced a surface cold front extending from South China all the way to northern Japan [*Hong Kong Observatory*, 2001]. Lifting of pollution ahead of the cold front over South China followed by westerly transport led to the highest eastward flux of CO in the lower FT over the western Pacific during the TRACE-P period, as diagnosed in the model (Figure 4). The TRACE-P DC-8 aircraft flew a sortie out of Hong Kong across the cold front on 7 March (Figure 5). Observed and simulated CO concentrations along the flight track are shown in Figure 5; simulated contributions from the Asian anthropogenic and biomass burning tracers are shown in Figure 6. The DC-8 aircraft headed north to (31°N, 125°E) and then east to (30°N, 140°E) to cross the front; it returned to Hong Kong along a southwest track and remained ahead of the front. The lifting of CO ahead of the cold front is manifest in the observations and is captured by the model, although the observations show that the high-CO plume extends to higher altitudes (5–8 km). Asian anthropogenic and biomass burning emissions make similar contributions to the CO frontal outflow in the model (Figure 6), as previously shown by *Bey et al.* [2001b]. Asian anthropogenic emissions are concentrated near the Pacific coast (Figure 1) and are thus directly swept southward by cold surges followed by lifting, while biomass burning effluents from Southeast Asia are transported northeastward in the BL prior to being lifted up at 25°–30°N along the Asian coast [*Bey et al.*, 2001b; *Liu et al.*, 2002]. We find in the model an enhanced outflow flux in the FT after all frontal passages. Such frontal outflow is generally confined between 2- to 6-km altitude and is maximum at ∼4 km. Lifting usually occurs over central and eastern China at 20°–35°N [*Miyazaki et al.*, 2003], and the plume travels northeastward along the WCB over the western Pacific, dissipating along the way. As the cold front moves over the ocean, the associated WCB may bring CO poor air masses from the BL up to the FT, contributing to the dilution of the Asian pollution plumes (C. Mari et al., The effect of clean warm conveyor belts on the export of pollution from East Asia, submitted to *Journal of Geophysical Research*, 2003).

[17] Associated with the frontal outflow in the FT ahead of the front is the BL continental outflow behind the front, capped at ∼2-km altitude by strong subsidence. This outflow contained high pollutant concentrations with CO levels in excess of 250 ppbv [*Carmichael et al.*, 2003] and was largely devoid of biomass burning influence. Figure 5 (bottom right) shows the BL outflow in the model on March 7. A subsequent DC-8 flight on 9 March investigated the evolution of this outflow over the western Pacific; the model shows it fanning out over the region as the front dissipates (Figure 7).

3.2. Convective Outflow

[18] Convection over East Asia varies seasonally, with maxima over the maritime continent in winter and over southern China in summer. During March–April, convection is largely restricted to Southeast Asia and increases in frequency during the period. Deep convection over Southeast Asia was primarily responsible for the continental outflow observed in the UT (7–12 km) at low latitudes (<35°N) during TRACE-P [*Li et al.*, 2003]. This convection is enhanced by extratropical forcing from the cold surge events [*Slingo*, 1998].

[19] We illustrate the convective outflow pattern with data from a DC-8 flight on 26–27 March out of Yokota Air Force Base. During 25–26 March a cold front passed over South China and migrated toward the South China Seas (Figure 4), while intense convective activity was developing over Southeast Asia. On 26–27 March the DC-8 aircraft took off from Yokota (36°N, 139°E) and sampled convective outflow along two extended walls (133°–139°E and 125°E). This convective outflow of Asian pollution in the middle and UT is seen in both the observations and the model (Figure 8, top and middle), although the DC-8 only

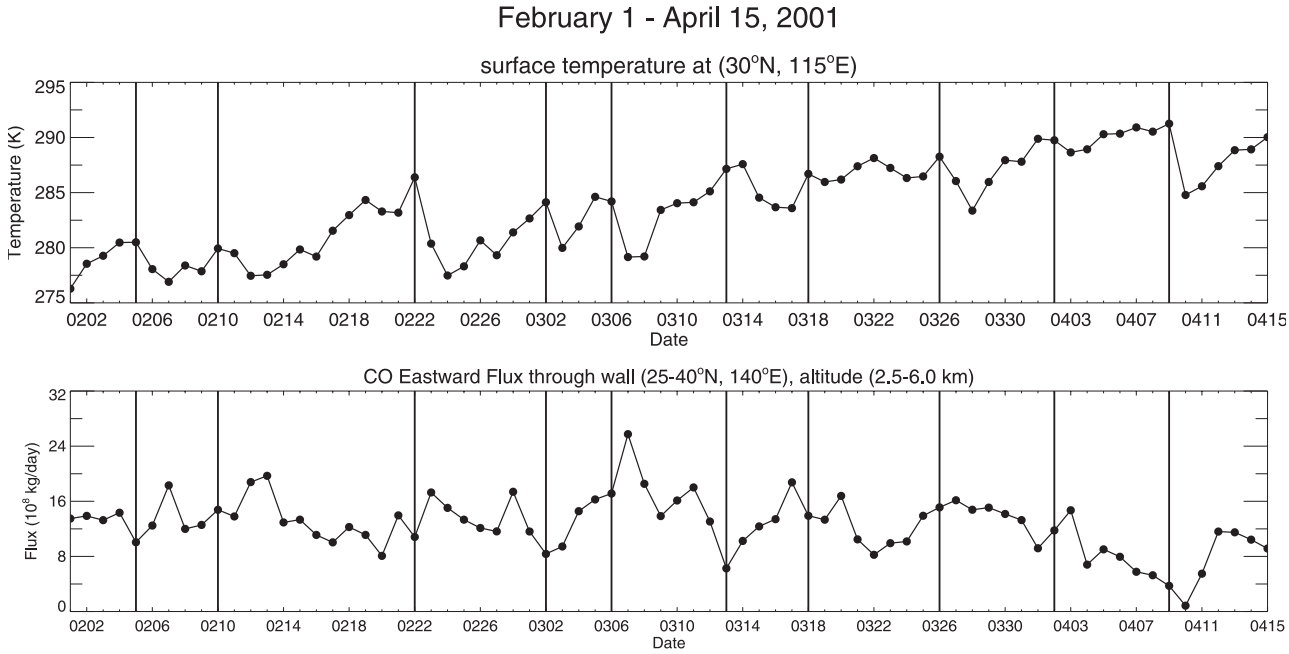

Figure 4. Cold frontal passages over China during 1 February–15 April 2001 and associated outflow of CO. The top panel shows the time series of Goddard Earth Observing System surface temperature at (30°N, 115°E). Cold fronts are identified by rapid increase in pressure (not shown) and decrease in temperature. The bottom panel shows the total simulated eastward flux of CO through a wall located at 140°E and extending from 25°–40°N and 2.5- to 6.0-km altitudes. Vertical lines indicate frontal passages.

crossed the edges of the plume. The tagged CO tracer simulation indicates that Asian biomass burning emissions dominated this convective outflow (Figure 8, bottom). The observed plumes in the lower troposphere near the end of the flight are missed by the model, reflecting the general inability of CTMs during TRACE-P to resolve deterministically the fine structure of Asian outflow in the BL [*Kiley et al.*, 2003]. We find in general that the UT convective events sampled during TRACE-P contained little anthropogenic influence.

3.3. European and African Contributions to Asian Outflow

[20] European anthropogenic pollution is transported to the Asian Pacific rim during spring in the lower troposphere around the Siberian anticyclone. The outflow associated with European pollution generally occurs during the cold surge events and is incorporated in the postfrontal BL outflow. Figure 9 shows such a case for 18 March when strong outflow in the BL was seen in both the observations and the model. This is one of the strongest contributions of European pollution found in the model along the flight tracks for the TRACE-P period, with an European CO enhancement of up to 45 ppbv (19% of total CO). The strongest event on 10 March corresponds to an European CO enhancement of up to 59 ppbv (18% of total CO). In both cases, and in general during TRACE-P, we find that European influences were systematically mixed with Asian pollution in the postal-frontal BL outflow and did not generate distinct CO plumes. Flights north of Japan (>40°N) would have been needed to obtain a detectable signal from European pollution.

[21] Biomass burning emissions from Africa contribute to the Asian outflow in the UT at <35°N latitude, but the corresponding CO enhancement is weak, <20 ppbv (21% of total CO) in our model at any time for the TRACE-P period. We could not find any event in the TRACE-P observations where a CO enhancement that is large enough to be detected would be attributable to African biomass burning.

3.4. Role of Topography

[22] Orographic forcing plays a major role in the large-scale lifting of Chinese pollution to the FT. Figure 10 shows the model monthly mean large-scale upward flux of Asian anthropogenic CO at 3-km altitude (sigma level 10 in GEOS3) in March 2001, with the terrain elevations superimposed. Plots for March of 1994, 1998, and 2000 all show similar centers of large-scale convergence in central and eastern China, as also previously noted by *Bey et al.* [2001b]. *Bey et al.* [2001b] proposed that the convergence reflects episodic lifting of pollution ahead of eastward moving cold fronts.

[23] We propose here orographic forcing as one other major process responsible for lifting of pollution to the FT over central and eastern China. We can see in Figure 10 that the ring of convergence around the North China Plain is associated with elevated terrain. The convergence maximum over the China coast is along the eastern edge of mountain ranges over South China, and the other locale of maximum convergence is the eastern flank of the Qinhai-Tibetan Plateau (including the Sichuan Basin). During cold surge events, northerly winds sweep anthropogenic effluents from the northern China plain which are then orographically lifted

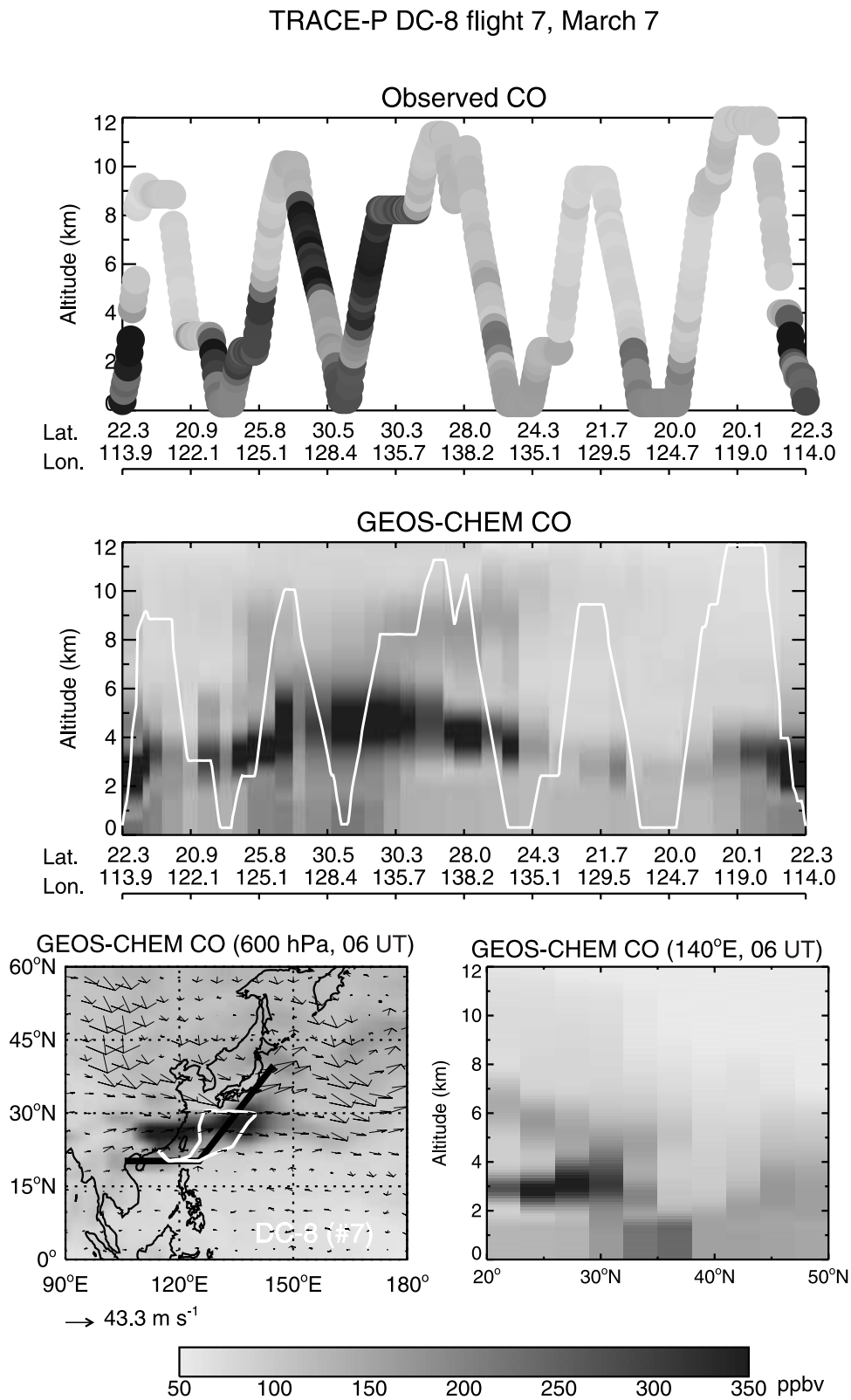

Figure 5. Frontal outflow in the lower free troposphere on 7 March 2001. DC-8 CO observations (top) are compared with model results (middle). The bottom left (map) shows the location of the surface cold front at 0600 UT (solid line), the DC-8 flight track (open line), wind vectors at 600 hPa, and simulated CO concentrations at 600 hPa. The bottom right shows the latitude-height cross section of the simulated CO at 140°E. See color version of this figure at back of this issue.

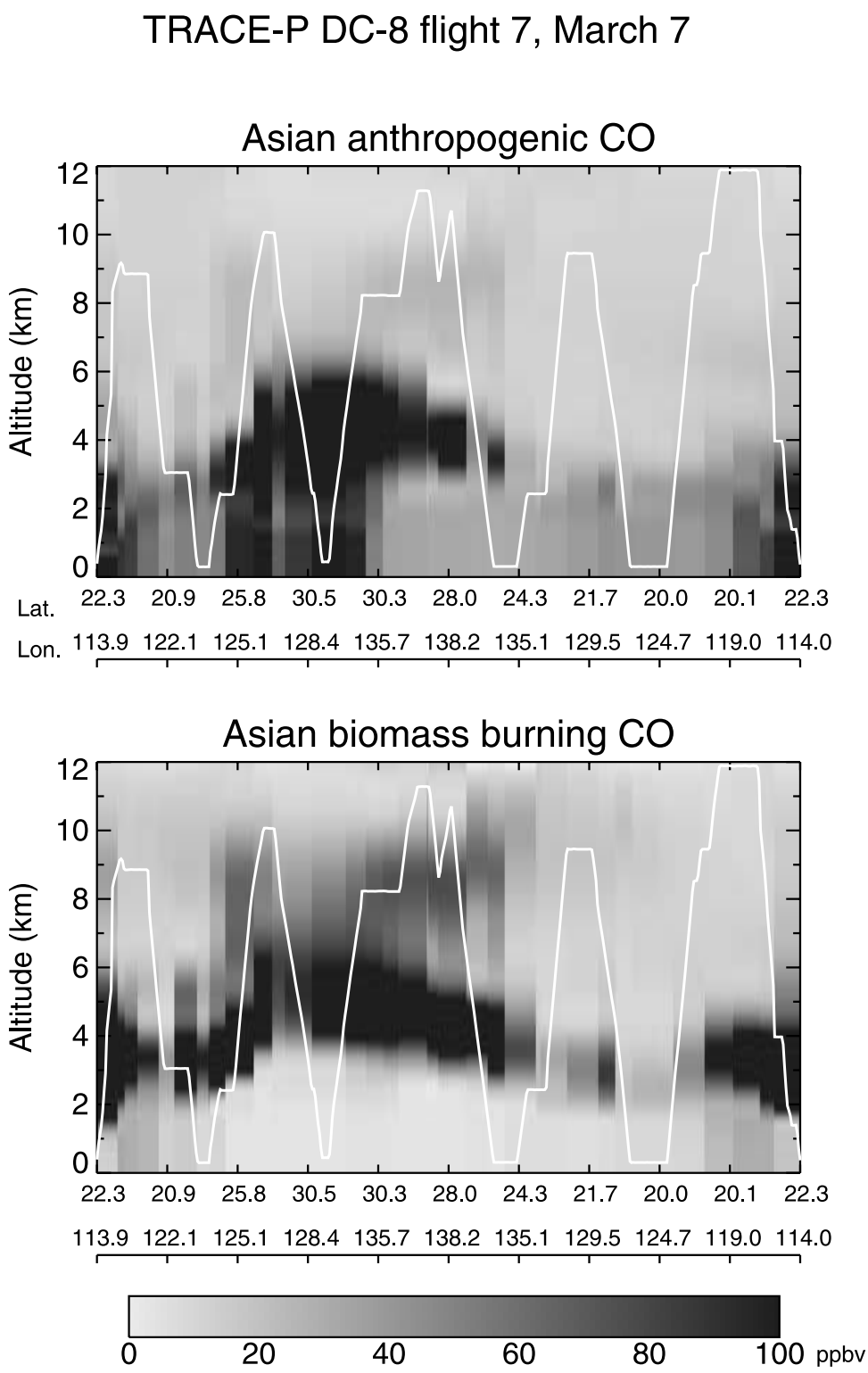

Figure 6. Simulated concentrations of Asian anthropogenic (top) and biomass burning (bottom) CO tracers along the DC-8 flight track (open line) on 7 March 2001. See color version of this figure at back of this issue.

to the FT over southern and central China. This explains why the region of maximum vertical flux in Figure 10 does not coincide with the region of maximum anthropogenic emission in northern China in Figure 1.

[24] The other possible role of topography in the export of Asian anthropogenic pollution to the western Pacific would concern emissions at high altitudes, where winds are stronger and more frequently westerly. One might expect high-altitude emissions to contribute disproportionately to the Asian outflow to the Pacific. We investigated this effect in the model by tagging separately emissions from different altitude bands and found it to be small, presumably because

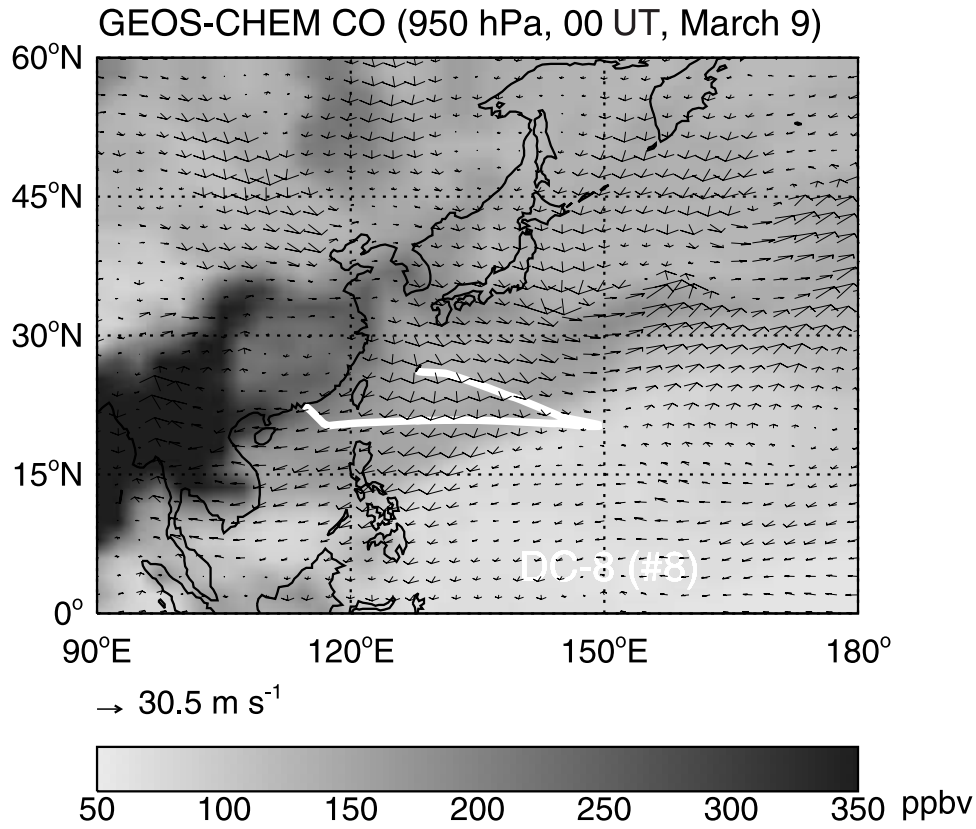

Figure 7. Simulated CO concentrations at 950 hPa on 9 March 2001, illustrating the boundary layer outflow of anthropogenic Asian pollution behind a cold front. Arrows are wind vectors, and the open line shows the DC-8 flight track. See color version of this figure at back of this issue.

of the long lifetime of CO and the eventual forcing of low-altitude emissions to the FT.

4. Interannual Variability of Transport Pathways

[25] We examined the interannual variability of Asian outflow to the Pacific with simulations for the springs of 1994, 1998, and 2000, in addition to the TRACE-P period. These years were chosen to cover the PEM-West B period (1994), as well as a major El Niño year (1998) and a La Niña year (2000) (Figure 11). During the 1994 spring (PEM-West B), no large anomalies in the Northern Hemispheric circulation affected the study region [*Merrill et al.*, 1997]. However, the Southern Oscillation Index (Figure 11) shows that the 1994 spring was affected by a weak El Niño episode, as discussed by *Goddard and Graham* [1997]. Asian outflow of CO to the Pacific in that spring was previously discussed by *Bey et al.* [2001b]. The 1998 spring was affected by one of the strongest Pacific El Niño episodes in the historical record [*Bell et al.*, 1999]. In contrast, the global climate in 2000 was influenced by the long-running Pacific La Niña episode that began in mid-1998 [*Lawrimore et al.*, 2001]. The 2001 spring was also categorized as La Niña [*Kousky et al.*, 2001].

[26] Using the 1979–1995 National Centers for Environmental Prediction/National Center for Atmospheric Research reanalysis in a study of climatology and interannual variation of the East Asian winter monsoon, *Zhang et al.* [1997] found that El Niño conditions and their immediate aftermaths were associated with a minimum in the frequency of cold surges across China. We find in the GEOS data that March 2001 (La Niña) features an unusually high frequency of cold surges, while March 1998 (El Niño) has a low frequency of cold surges. During El Niño, there is a pronounced eastward extension of deep tropical convection from the western Pacific to the central and eastern Pacific [*Philander*, 1990]. We find in the GEOS data that convection in Southeast Asia tends to be suppressed during El Niño and enhanced during La Niña, consistent with the Tropical Rainfall Measuring Mission precipitation patterns (TRMM) (available at http://trmm.gsfc.nasa.gov/images_dir/avg_rainrate.html).

[27] Figure 12 shows the latitude-altitude cross sections at 140°E of monthly mean Asian CO concentrations for March of 1994, 1998, and 2000. The same plot for March 2001 was presented earlier in Figure 3. In all years, Asian pollution influence is strongest at 30°–45°N in the BL and at 20°–35°N in the lower FT, and features the same relative contributions from anthropogenic and biomass burning sources as discussed previously in section 3. Outflow in the lower FT was strongest in 1998, while outflow in the UT was particularly strong in 2001. Relative to the PEM-West B period, TRACE-P features stronger outflow in the BL and UT, weaker in the middle troposphere (2–8 km).

[28] Figure 13 shows monthly mean horizontal fluxes of Asian biomass burning and anthropogenic CO, integrated

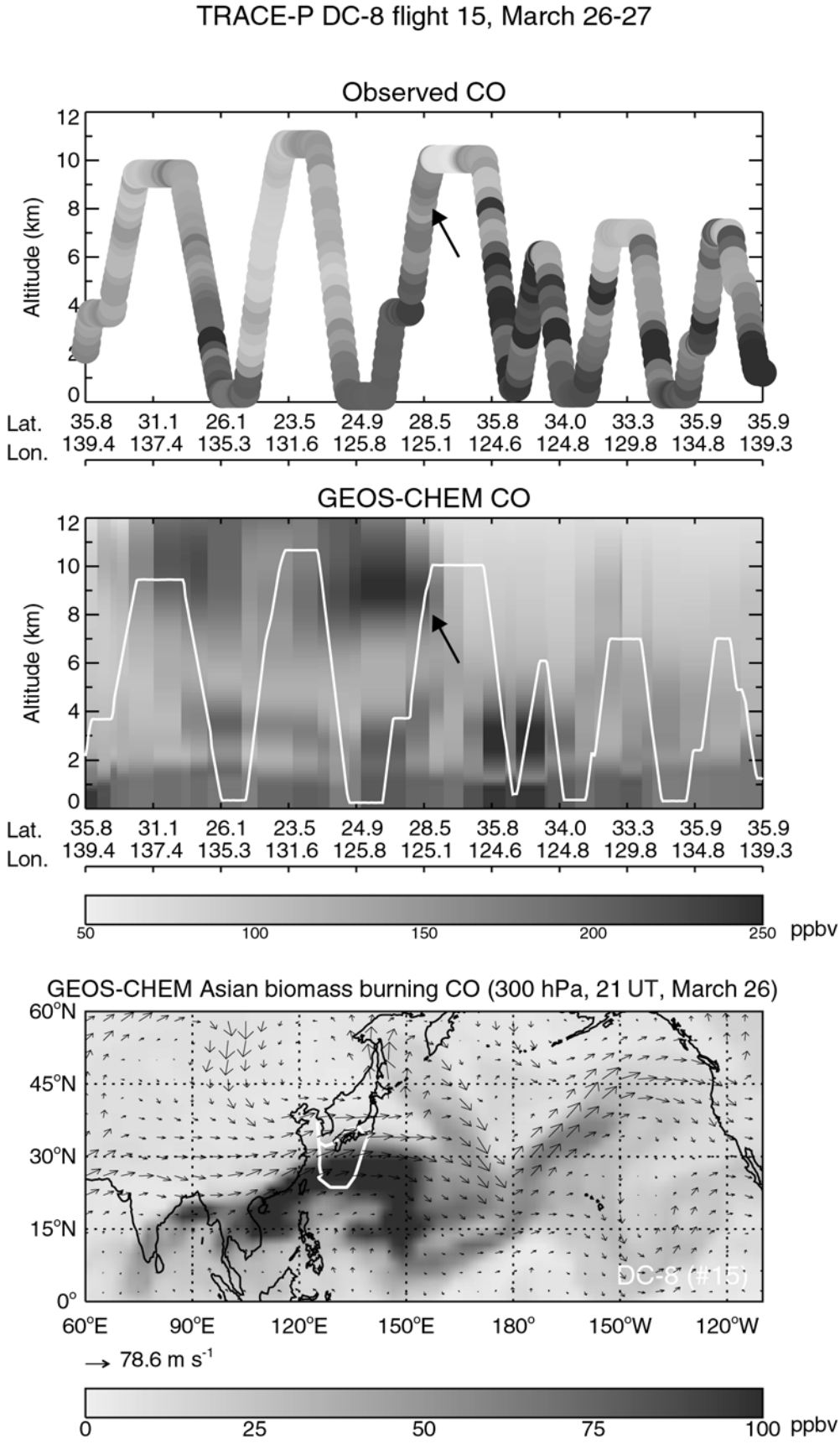

Figure 8. Convective outflow of Asian biomass burning CO in the upper troposphere on 26–27 March 2001. DC-8 CO observations (top) are compared with model results (middle). The bottom shows model Asian biomass burning CO concentrations at 300 hPa and 2100 UT, March 26. The open lines are the DC-8 flight track. Arrows in the top and middle indicate convective outflow. Arrows on the map are wind vectors. See color version of this figure at back of this issue.

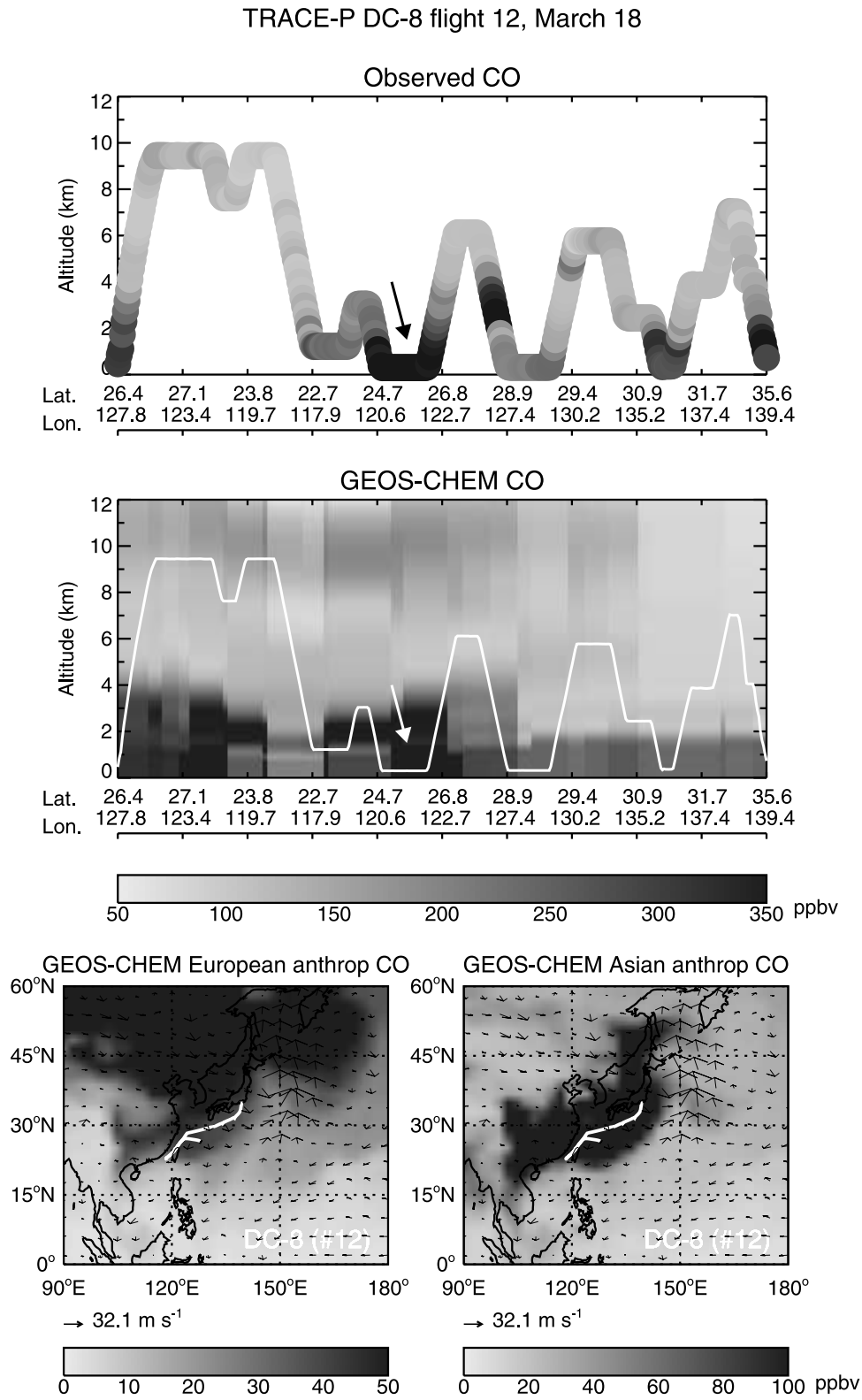

Figure 9. Postfrontal boundary layer outflow of Asian and European pollution on 18 March 2001. DC-8 CO observations (top) are compared with model results (middle) sampled along the DC-8 flight track (open line, bottom). The bottom shows the simulated concentrations of the European (bottom left) and Asian (bottom right) anthropogenic CO tracers at 950 hPa. Arrows in the top and middle indicate strong outflow in the boundary layer. Arrows on the map are wind vectors. See color version of this figure at back of this issue.

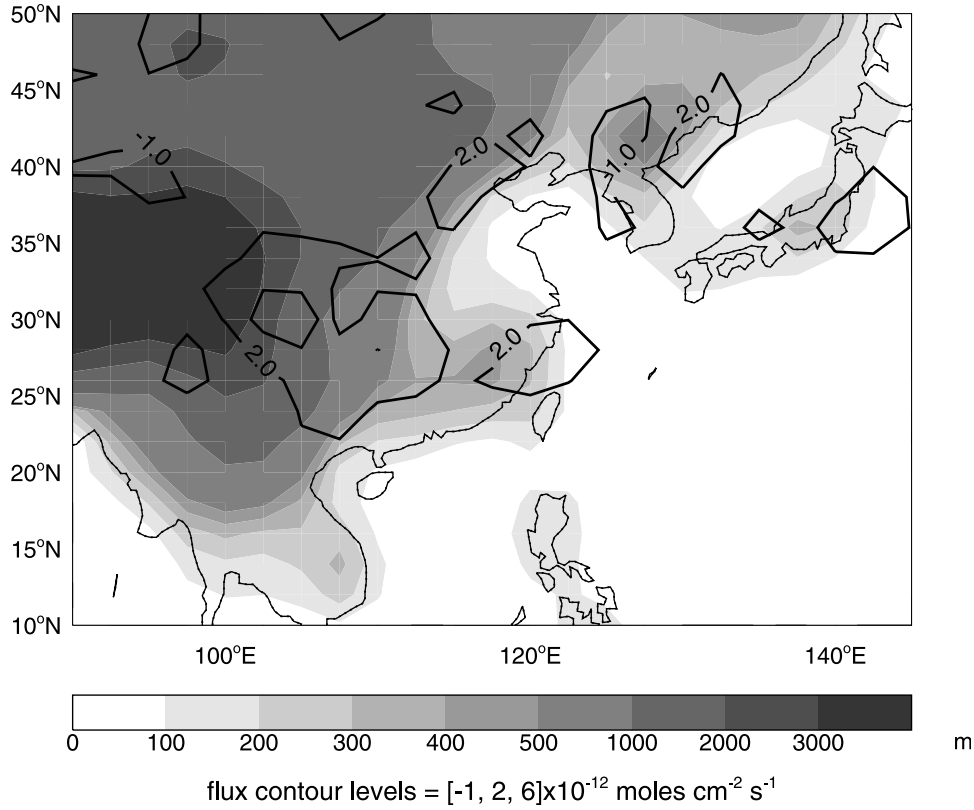

Figure 10. Monthly mean large-scale vertical flux (line contours, 10^{-12} moles cm^{-2} s^{-1}) at 3-km altitude of Asian anthropogenic CO in March 2001. Filled contours show the terrain elevations.

over the BL (1000–700 hPa) for March of all four years. The BL outflow of biomass burning CO to the Pacific is negligible for all years (Figure 13a). During March 1998 (El Niño), the suppression of convection in Southeast Asia results in a large flux northeastward in the BL to the convergence region near 25°–30°N, where lifting into the lower FT takes place by the mechanism discussed in section 3.1. During March 2001 (La Niña), frequent deep convection over Southeast Asia preferentially transports biomass burning CO to the UT, limiting the northeastward transport in the BL. The TRACE-P mission took place in a year when the role of convection was above normal [*Fuelberg et al.*, 2003]. However, we find that for all years except 1998, deep convection south of 22°N was the

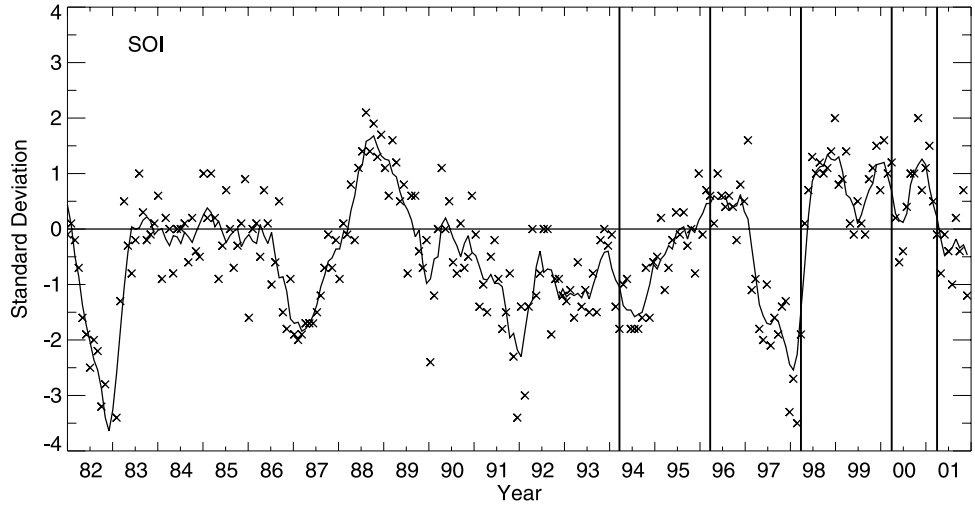

Figure 11. Five-month running mean of the Southern Oscillation Index from the NOAA Climate Prediction Center. Negative values indicate El Niño conditions. Vertical lines indicate our 5 simulation years: 1994 (Pacific Exploratory Mission-West B), 1996, 1998, 2000, and 2001 (Transport and Chemical Evolution over the Pacific).

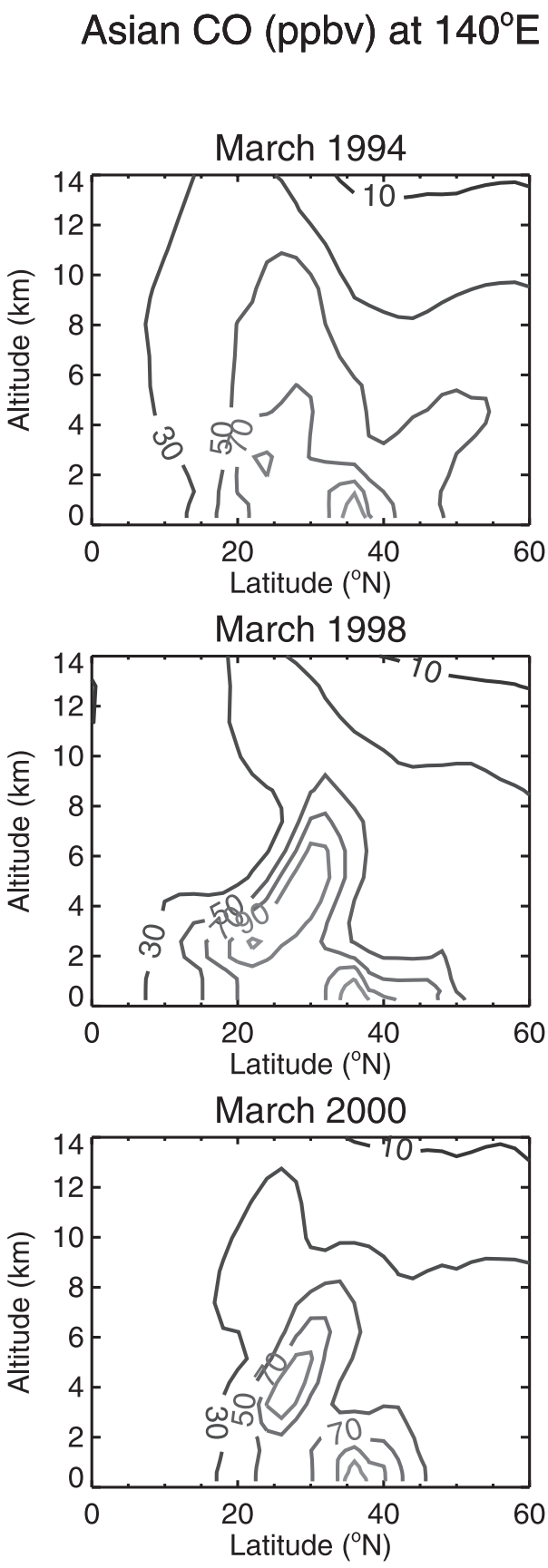

Figure 12. Same as Figure 3, but for March of 1994, 1998, and 2000.

most important mechanism for lifting biomass burning emissions into the FT.

[29] A remarkable feature in Figure 13b is the unusually strong BL outflow of Asian anthropogenic sources over the western Pacific during 2001, reflecting the strong surface Siberian high and high frequency of cold surges typical of La Niña conditions. By contrast, weak BL outflow is seen under the March 1994 and 1998 El Niño conditions when cold surge events were less frequent.

5. Seasonal Variability of Asian Outflow to the Pacific

[30] The seasonal variation in the climate of eastern Asia is largely related to the monsoon system [*Ding*, 1994]. We examine here the seasonal variation in Asian outflow of CO to the Pacific for the year 1996. We previously used this year to investigate the seasonal variation in outflow of ozone [*Liu et al.*, 2002]. La Niña conditions persisted across the tropical Pacific from November 1995 through May 1996, with near-normal conditions during the rest of the year [*Halpert and Bell*, 1997] (Figure 11). Figure 14 shows the seasonally averaged horizontal fluxes of Asian anthropogenic CO for the 1000- to 750-hPa column and at 200 hPa. In winter, Asian CO is trapped in the BL by the large-scale subsidence over the Asian continent. The strong northwesterly (>25°N) monsoon combines with high anthropogenic emissions in northeastern Asia, leading to large CO fluxes in the BL off the East Asian coast. The northeasterly monsoon (<25°N) sweeps this pollution further southward into the tropics, where it is lifted up into the UT by deep convection over the maritime continent and is subsequently transported northward (the upper branch of the local Hadley circulation) into the midlatitude westerlies [*Newell et al.*, 1997; *Liu et al.*, 2002].

[31] In summer the southerly and southwesterly monsoon winds prevail over eastern China south of 40°N [*Ding*, 1994]. This monsoonal flow transports Asian pollution toward the northeast (Figure 14a), during which period the pollution may be subject to frequent lifting into the UT by deep convection. In the UT a large fraction of upwelled Asian pollution circulates southward and then westward around the Tibetan anticyclone (South Asia high), resulting in outflow toward the Middle East rather than to the Pacific [*Liu et al.*, 2002; *Lelieveld et al.*, 2002] (Figure 14b). This transport pathway has important implications for the export of Asian pollution to the Pacific, as discussed below. In the middle troposphere, the Tibetan anticyclone is much weaker and most of Asian pollution is transported to the Pacific in the midlatitude westerlies (not shown).

[32] While the monsoonal flow may reach deep into northern China in July, it begins to weaken in August, and by October it is completely replaced by the winter northeasterly flow [*Ding*, 1994]. This northeasterly flow extends to the South China coast, contrasting with the reverse flow in spring (Figure 14a).

[33] Figure 15 shows the seasonal variation in the total Asian outflow flux of CO to the Pacific (eastward flux of CO integrated for the 1000- to 200-hPa column through a wall at 150°E between 10° and 60°N). Contributions from different sources to this outflow are identified. The magnitude of the Asian outflow flux varies seasonally by a factor

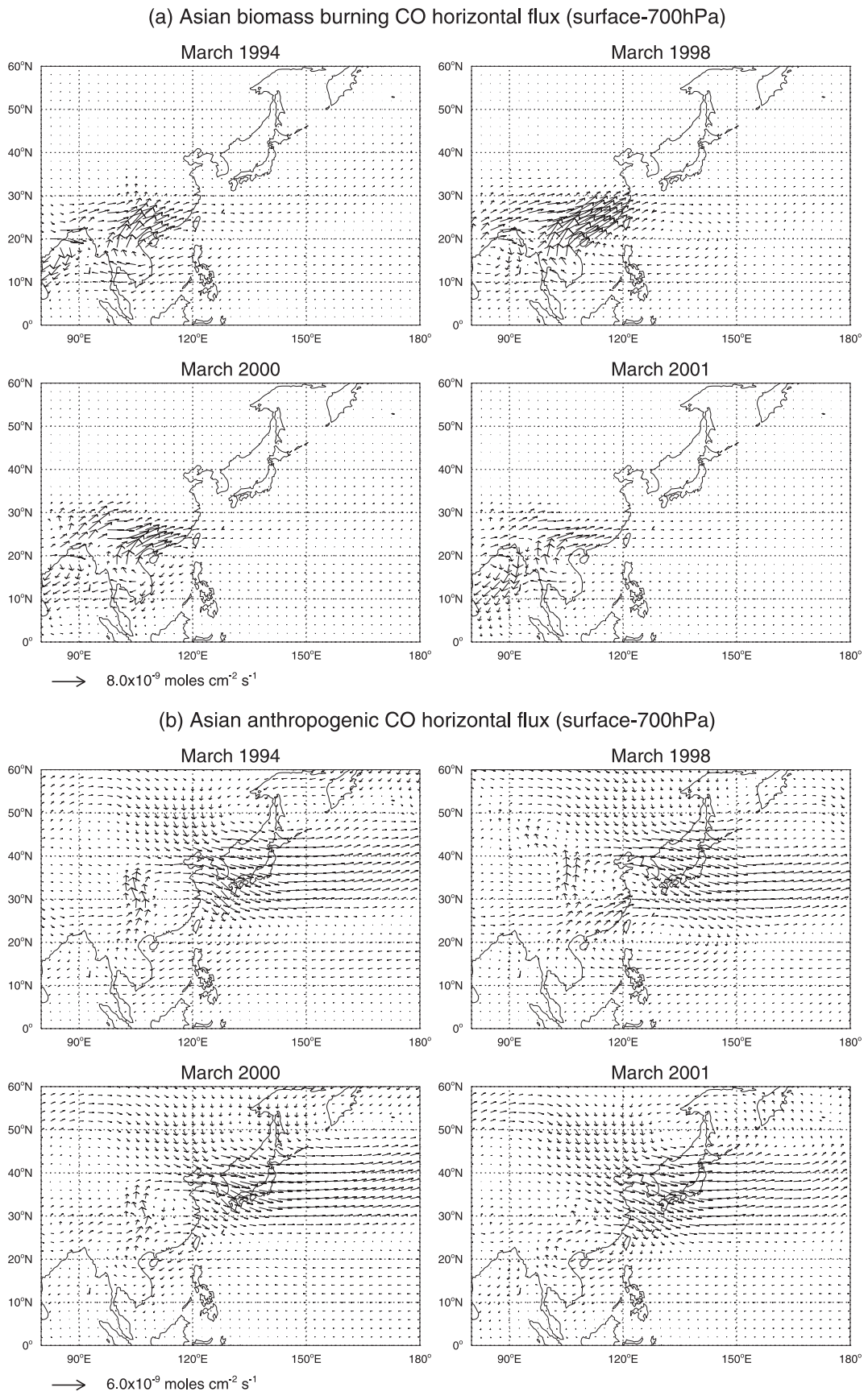

Figure 13. (a) Monthly mean horizontal fluxes of Asian biomass burning CO in March, shown for the 1000- to 700-hPa column and for 1994, 1998, 2000, and 2001, respectively. (b) Same as Figure 13a but for Asian anthropogenic CO. See color version of this figure at back of this issue.

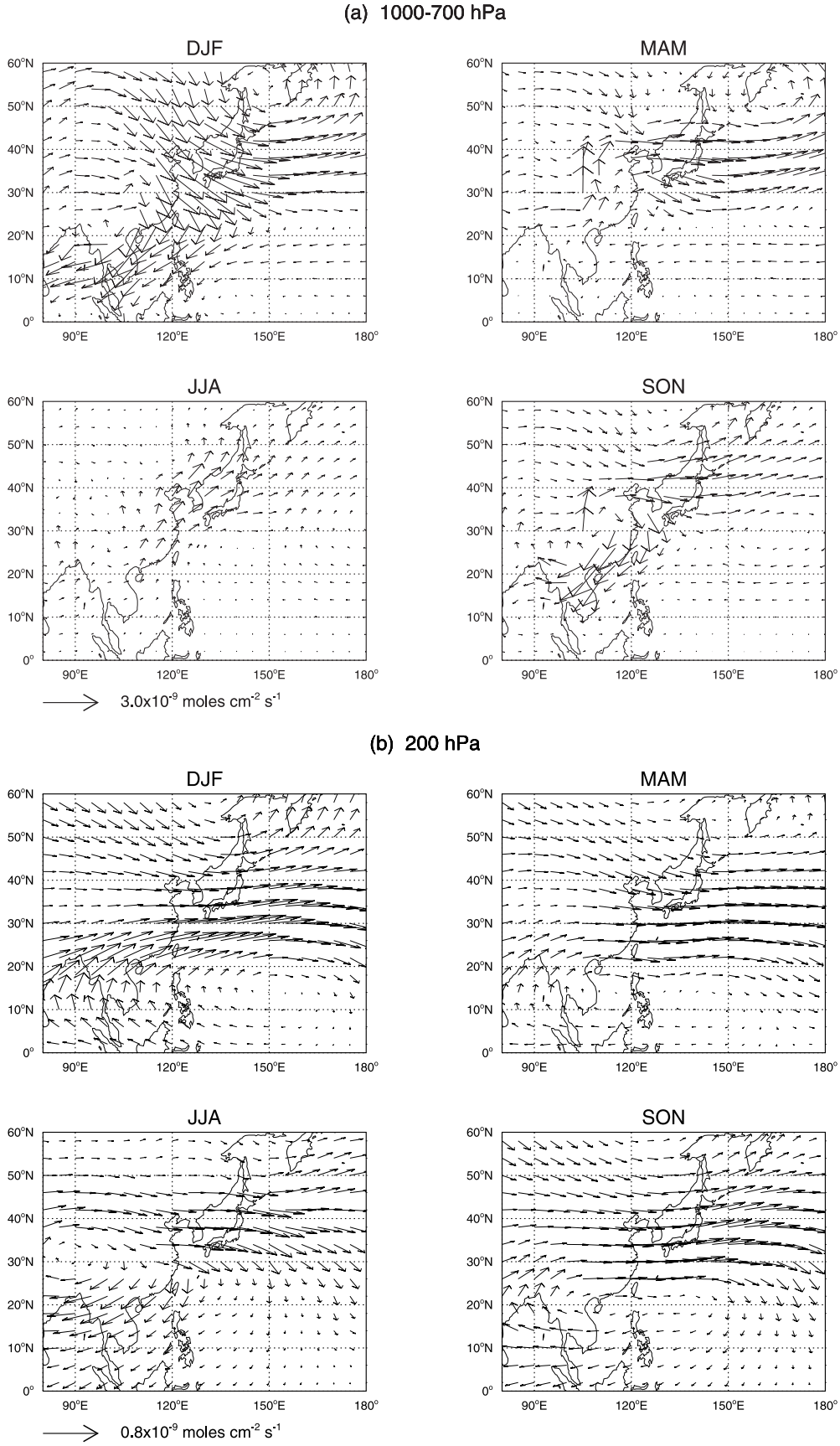

Figure 14. Horizontal fluxes of Asian anthropogenic CO, shown for (a) 1000- to 750-hPa column and (b) 200 hPa. Values are seasonal model averages for 1996. See color version of this figure at back of this issue.

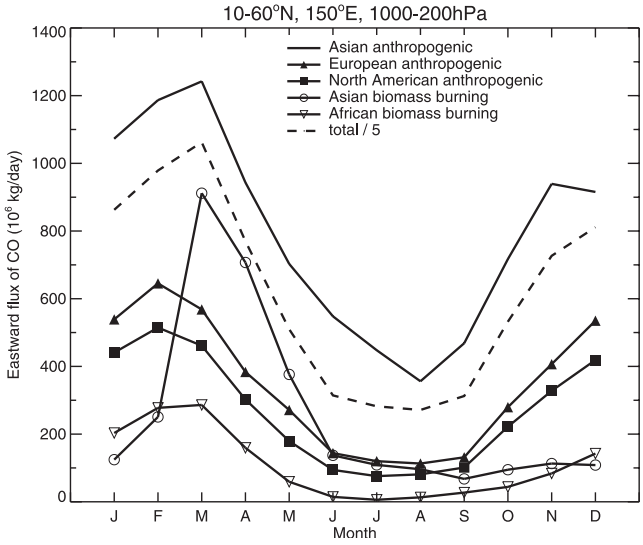

Figure 15. Contributions from different sources to the Asian outflow of CO over the Pacific as a function of season in 1996. The Asian outflow flux is defined as the eastward flux (10^6 kg day^{-1}) integrated for the 1000- to 200-hPa column through a wall located at 150°E between 10° and 60°N. Contributions from individual sources (i.e., Asian anthropogenic, European anthropogenic, North American anthropogenic, Asian biomass burning, African biomass burning) are determined by a tagged CO tracer simulation. The total Asian outflow flux of CO (scaled down by a factor of 5) is plotted as a dashed line. All values are monthly averages.

of 3–4 with a maximum in January–March and a minimum in summer; the latter reflects the monsoonal ventilation to the UT followed by easterly flow away from the Pacific (as discussed above) as well as low background concentration of CO in summer. The Asian biomass burning contribution is maximum in March–April and much less significant in other seasons. The African biomass burning contribution, which is much smaller, is maximum in January–March. European and North American anthropogenic contributions also peak in January–March.

[34] Anthropogenic CO sources in Asia make the largest contribution to the Asian outflow flux of CO over the Pacific in all seasons (Figure 15). European anthropogenic sources contribute more to the Asian outflow flux of CO than North American sources, whereas for ozone we found the reverse [*Liu et al.*, 2002]. Intercontinental transport of North American ozone is promoted by more efficient lifting of North American than European pollution to the FT [*Stohl*, 2001] where ozone has a much longer lifetime (weeks) than in the BL (days).

6. Summary and Conclusions

[35] We have used a global 3-D chemical tracer model driven by assimilated meteorological observations to examine transport pathways for Asian pollution outflow over the western Pacific. Our focus was to interpret and generalize the observations from the TRACE-P aircraft mission in February–April 2001. We placed a particular emphasis on putting the TRACE-P results in an interannual and seasonal context. Carbon monoxide (CO) was used as a long-lived combustion tracer. It has major contributions from both fossil fuel and seasonal biomass burning in Southeast Asia in spring. Tagged CO tracers in the model allowed us to examine the contributions from different source regions to the Asian outflow.

[36] The major process responsible for the export of Asian anthropogenic pollution (fossil fuel and biofuel) to the western Pacific during spring is frontal lifting to the free troposphere (FT) ahead of southeastward moving cold fronts (the leading edges of cold surges) and transport in the boundary layer (BL) behind the cold front. Orographic lifting over central and eastern China combines with the cold fronts to promote the transport of Chinese pollution to the FT. Biomass burning effluents from Southeast Asia are lifted in the warm conveyor belt (WCB) ahead of the front, mixing with the anthropogenic pollution in the FT outflow. However, we find that deep convection is a more important mechanism than frontal lifting for driving export of biomass burning effluents from Southeast Asia. The postfrontal BL outflow sampled in TRACE-P was largely devoid of biomass burning influence.

[37] Frontal outflow to the NW Pacific is maximum at 20°–35°N and generally confined between 2- to 6-km altitude (maximum at ~4-km altitude), whereas the BL outflow is strongest at 30°–45°N. Convective outflow typically takes place at 7- to 12-km altitude and at low latitudes (<35°N). During TRACE-P, convective events tended to occur with a similar periodicity (~7 days) as the cold fronts, reflecting extratropical forcing of tropical convection by the cold surge events.

[38] A large fraction of Asian anthropogenic emissions is released at high elevation (35% above 0.5-km altitude). However, we did not find a significant preferential contribution of high-altitude emissions to Asian outflow over the Pacific, despite stronger westerly winds at higher altitude. This result probably reflects the long lifetime of CO and the eventual forcing of low-altitude emissions to the FT.

[39] We examined the contributions from European and African (biomass burning) sources to the Asian outflow of pollution over the western Pacific. European pollution is transported to the Asian Pacific rim in the lower troposphere around the Siberian anticyclone and mixes with Asian pollution in the BL outflow; south of 40°N, it does not generate a distinct signal (<60 ppbv CO) because of the superposition of the much larger Asian contribution. African biomass burning effluents are transported to the western Pacific in the upper troposphere (UT) by the subtropical jet, but the signal in the model is faint (never more than 20 ppbv CO) and it could not be detected in any of the TRACE-P flights.

[40] Interannual variability in springtime Asian outflow was examined by comparing CO simulations for 1994 (weak El Niño), 1998 (El Niño), 2000 (La Niña), and 2001 (La Niña). The dominant outflow pathways are similar for all years, but there is some interannual variability related to ENSO. El Niño conditions are associated with a weakened Siberian high, a lower frequency of cold surges, and suppressed convection over Southeast Asia. Spring 2001 (TRACE-P) experienced unusually strong convection in Southeast Asia with associated lifting of biomass burning

effluents to the UT and an unusually high frequency of cold surges which led to much stronger BL outflow of Asian pollution than in 1994 (PEM-West B).

[41] Seasonal variability in mechanisms for pollution transport in East Asia is largely related to the monsoon system. In winter, Asian pollution is capped in the BL by the general subsidence over the Asian continent and is swept by northerly monsoons southward into the tropics. In summer, Asian pollution is transported northeastward by the monsoon and is subject to frequent lifting into the UT by deep convection. In the UT a large part of this upwelled pollution circulates southward and then westward around the Tibetan anticyclone, heading toward the Middle East rather than to the Pacific. Spring and fall are meteorologically transitional periods with frequent cold fronts. In fall the building continental high (winter monsoon) sweeps pollution southward to relatively low latitudes where they are lifted up into the FT by convection and cold fronts. In spring, convection over Asian continent in particular at lower latitudes starts to rise, and Southeast Asian biomass burning is at its seasonal maximum in this season. Examination of the seasonal variability of the Asian outflow flux of CO to the Pacific indicates that the flux varies seasonally by a factor of 3–4 (maximum in March and minimum in summer). The March maximum results from frequent cold surge events and seasonal biomass burning emissions. The summer minimum reflects the monsoonal ventilation to the UT followed by easterly flow away from the Pacific as well as low background concentration of CO in summer.

[42] **Acknowledgments.** This work was supported by the NASA Global Tropospheric Chemistry Program. We thank Henry Fuelberg, Rene Garreaud, Celine Mari, Paul Palmer, Brad Pierce, and Andreas Stohl for useful discussions and Wen Lam Chang for providing daily weather maps for the springs of 1994–2001.

References

Allen, D. J., R. B. Rood, A. M. Thompson, and R. D. Hudson, Three-dimensional radon 222 calculations using assimilated meteorological data and a convective mixing algorithm, *J. Geophys. Res.*, *101*, 6871–6881, 1996.

Arakawa, A., and W. H. Schubert, Interaction of cumulus cloud ensemble with the large-scale environment, part I, *J. Atmos. Sci.*, *31*, 671–701, 1974.

Banic, C. M., G. A. Isaac, H. R. Cho, and J. V. Iribane, The distribution of pollutants near a frontal surface: A comparison between field experiment and modeling, *Water Air Soil Pollut.*, *30*, 171–177, 1986.

Bell, G. D., M. S. Halpert, C. F. Ropelewski, V. E. Kousky, A. V. Douglas, R. C. Schnell, and M. E. Gelman, Climate assessment for 1998, *Bull. Am. Meteorol. Soc.*, *80*, s1–s48, 1999.

Bethan, S., G. Vaughan, C. Gerbig, A. Volz-Thomas, H. Richer, and D. A. Tiddeman, Chemical air mass differences near fronts, *J. Geophys. Res.*, *103*, 13,413–13,434, 1998.

Bey, I., D. J. Jacob, R. M. Yantosca, J. A. Logan, B. Field, A. M. Fiore, Q. Li, H. Liu, L. J. Mickley, and M. Schultz, Global modeling of tropospheric chemistry with assimilated meteorology: Model description and evaluation, *J. Geophys. Res.*, *106*, 23,073–23,096, 2001a.

Bey, I., D. J. Jacob, J. A. Logan, and R. M. Yantosca, Asian chemical outflow to the Pacific in spring: Origins, pathways, and budgets, *J. Geophys. Res.*, *106*, 23,097–23,114, 2001b.

Boyle, J. S., and T.-J. Chen, Synoptic aspects of the wintertime East Asian monsoon, in *Monsoon Meteorology*, edited by C. P. Chang and T. N. Krishnamurti, pp. 125–160, Oxford Univ. Press, New York, 1987.

Brown, R. M., P. H. Daum, S. E. Schwartz, and M. R. Hjelmfelt, Variations in the chemical composition of clouds during frontal passage, in *The Meteorology of Acid Deposition*, edited by P. J. Samson, pp. 202–212, Air Pollut. Control Assoc., Pittsburgh, Pa., 1984.

Carmichael, G. R., I. Uno, M. J. Phadnis, Y. Zhang, and Y. Sunwoo, Tropospheric ozone production and transport in the springtime in east Asia, *J. Geophys. Res.*, *103*, 10,649–10,671, 1998.

Carmichael, G. R., et al., Regional-scale chemical transport modeling in support of intensive field experiments: Overview and analysis of the Tropospheric Experiment Transport and Chemical Evolution over the Pacific observations, *J. Geophys. Res.*, *108*(D21), 8823, doi:10.1029/2002JD003117, in press, 2003.

Compo, G. P., et al., The horizontal and vertical structure of east Asian winter monsoon pressure surges, *Q. J. R. Meteorol. Soc.*, *125*, 29–54, 1999.

Cooper, O. R., J. L. Moody, D. D. Parrish, M. Trainer, T. B. Ryerson, J. S. Holloway, G. Hübler, F. C. Fehsenfeld, S. J. Oltmans, and M. J. Evans, Trace gas signatures of the airstreams within North Atlantic cyclones: Case studies from the North Atlantic Regional Experiment (NARE '97) aircraft intensive, *J. Geophys. Res.*, *106*, 5437–5456, 2001.

Dickerson, R. R., et al., Thunderstorms—An important mechanism in the transport of air pollutants, *Science*, *235*, 460–464, 1987.

Ding, Y., Build-up, air mass transformation and propagation of the Siberian High and its relation to cold surge in East Asia, *Meteorol. Atmos. Phys.*, *44*, 281–292, 1990.

Ding, Y. H., *Monsoons over China*, Kluwer Acad., Norwell, Mass., 1994.

Donnell, E. A., D. J. Fish, E. M. Dicks, and A. J. Thorpe, Mechanisms for pollutant transport between the boundary layer and the free troposphere, *J. Geophys. Res.*, *106*, 7847–7856, 2001.

Duncan, B. N., R. V. Martin, A. C. Staudt, R. M. Yevich, and J. A. Logan, Interannual and seasonal variability of biomass burning emissions constrained by satellite observations, *J. Geophys. Res.*, *108*(D2), 4100, doi:10.1029/2002JD002378, 2003.

Fuelberg, H. E., C. Kiley, J. R. Hannan, D. J. Westberg, M. A. Avery, and R. E. Newell, Meteorological conditions and transport pathways during the transport and chemical evolution over the Pacific experiment, *J. Geophys. Res.*, *108*(D20), 8782, doi:10.1029/2002JD003092, in press, 2003.

Garreaud, R. D., Subtropical cold surges: Regional aspects and global distribution, *Int. J. Climatol.*, *21*, 1181–1197, 2001.

Goddard, L., and N. E. Graham, El Niño in the 1990s, *J. Geophys. Res.*, *102*, 10,423–10,436, 1997.

Halpert, M. S., and G. D. Bell, Climate assessment for 1996, *Bull. Am. Meteorol. Soc.*, *78*, s1–s49, 1997.

Heald, C., D. J. Jacob, P. I. Palmer, M. J. Evans, G. W. Sachse, H. Singh, and D. Blake, Biomass burning emission inventory with daily resolution: Application to aircraft observations of Asian outflow, *J. Geophys. Res.*, *108*(D21), 8811, doi:10.1029/2002JD003082, in press, 2003.

Hong Kong Observatory, Monthly weather summary, Hong Kong, China, 2001.

Jacob, D. J., J. Crawford, M. M. Kleb, V. S. Connors, R. J. Bendura, J. L. Raper, G. W. Sachse, J. Gille, L. Emmons, and C. Heald, Transport and chemical evolution over the Pacific mission: Design, execution, and first results, *J. Geophys. Res.*, *108*(D20), 8781, doi:10.1029/2002JD003276, in press, 2003.

Kiley, C., et al., An intercomparison and evaluation of aircraft-derived and simulated CO from seven chemical transport models during the Transport and Chemical Evolution over the Pacific experiment, *J. Geophys. Res.*, *108*(D21), 8819, doi:10.1029/2002JD003089, in press, 2003.

Kousky, V. E., , G. D. Bell, M. S. Halpert, and W. Higgins (Eds.), Climate diagnostics bulletin, *Bull. 01/3*, pp. 3–7, Clim. Predict. Cent., Natl. Cent. for Environ. Predict., Natl. Oceanic and Atmos. Admin., Camp Springs, Md., 2001.

Kowol-Santen, J., M. Beekmann, S. Schmitgen, and K. Dewey, Tracer analysis of transport from the boundary layer to the free troposphere, *Geophys. Res. Lett.*, *28*, 2907–2910, 2001.

Lawrimore, J. H., et al., Climate assessment for 2000, *Bull. Am. Meteorol. Soc.*, *82*, s51–s55, 2001.

Lelieveld, J., et al., Global air pollution crossroads over the Mediterranean, *Science*, *298*, 794–799, 2002.

Li, Q., D. J. Jacob, R. Yantosca, C. Heald, H. Singh, M. Koike, Y. Zhao, G. W. Sachse, and D. Streets, A global three-dimensional model analysis of the atmospheric budgets of HCN and CH_3CN: Constraints from aircraft and ground measurements, *J. Geophys. Res.*, *108*(D21), 8827, doi:10.1029/2002JD003075M, in press, 2003.

Lin, S.-J., and R. B. Rood, Multidimensional flux-form semi-Lagrangian transport schemes, *Mon. Weather Rev.*, *124*, 2046–2070, 1996.

Liu, H., D. J. Jacob, L. Y. Chan, S. J. Oltmans, I. Bey, R. M. Yantosca, J. M. Harris, B. N. Duncan, and R. V. Martin, Sources of tropospheric ozone along the Asian Pacific Rim: An analysis of ozonesonde observations, *J. Geophys. Res.*, *107*(D21), 4573, doi:10.1029/2001JD002005, 2002.

Merrill, J. T., R. E. Newell, and A. S. Bachmeier, A meteorological overview for the Pacific Exploratory Mission-West Phase B, *J. Geophys. Res.*, *102*, 28,241–28,253, 1997.

Miyazaki, Y., et al., Synoptic-scale transport of reactive nitrogen over the western Pacific in spring, *J. Geophys. Res.*, *108*(D20), 8788, doi:10.1029/2002JD003248, in press, 2003.

Moorthi, S., and M. J. Suarez, Relaxed Arakawa-Schubert: A parameterization of moist convection for general circulation models, *Mon. Weather Rev.*, *120*, 978–1002, 1992.

Newell, R. E., and M. J. Evans, Seasonal changes in pollutant transport to the North Pacific: The relative importance of Asian and European sources, *Geophys. Res. Lett.*, *27*, 2509–2512, 2000.

Newell, R. E., E. V. Browell, D. D. Davis, and S. C. Liu, Western Pacific tropospheric ozone and potential vorticity: Implications for Asian pollution, *Geophys. Res. Lett.*, *24*, 2733–2736, 1997.

Palmer, P. I., D. J. Jacob, D. B. Jones, C. Heald, R. Yantosca, J. A. Logan, G. W. Sachse, and D. Streets, Inverting for emissions of carbon monoxide from Asia using aircraft observations over the western Pacific, *J. Geophys. Res.*, *108*(D21), 8828, doi:10.1029/2003JD003397, in press, 2003.

Philander, S. G., *El Niño, La Niña, and the Southern Oscillation*, Academic, San Diego, Calif., 1990.

Pickering, K. E., A. M. Thompson, J. R. Scala, W.-K. Tao, R. R. Dickerson, and J. Simpson, Free tropospheric ozone production following entrainment of urban plumes into deep convection, *J. Geophys. Res.*, *97*, 17,985–18,000, 1992.

Sachse, G. W., G. F. Hill, L. O. Wade, and M. G. Perry, Fast-response, high-precision carbon-monoxide sensor using a tunable diode-laser absorption technique, *J. Geophys. Res.*, *92*, 2071–2081, 1987.

Schneider, H. R., D. B. A. Jones, M. B. McElroy, and G.-Y. Shi, Analysis of residual mean transport in the stratosphere: 1. Model description and comparison with satellite data, *J. Geophys. Res.*, *105*, 19,991–20,011, 2000.

Slingo, J. M., Extratropical forcing of tropical convection in a northern winter simulation with the UGAMP GCM, *Q. J. R. Meteorol. Soc.*, *124*, 27–51, 1998.

Staudt, A. C., D. J. Jacob, J. A. Logan, D. Bachiochi, T. N. Krishnamurti, and G. W. Sachse, Continental sources, transoceanic transport, and interhemispheric exchange of carbon monoxide over the Pacific, *J. Geophys. Res.*, *106*, 32,571–32,590, 2001.

Stohl, A., A 1-year Lagrangian "climatology" of airstreams in the Northern Hemisphere troposphere and lowermost stratosphere, *J. Geophys. Res.*, *106*, 7263–7279, 2001.

Streets, D., et al., An inventory of gaseous and primary aerosol emissions in Asia in the year 2000, *J. Geophys. Res.*, *108*(D21), 8809, doi:10.1029/2002JD003093, in press, 2003.

Takacs, L. L., A. Molod, and T. Wang, Documentation of the Goddard Earth Observing System (GEOS) general circulation model—version 1, *NASA Tech. Memo., TM-104606*, *1*, 100 pp., 1994.

Yienger, J. J., M. Galanter, T. A. Holloway, M. J. Phadnis, S. K. Guttikunda, G. R. Carmichael, W. J. Moxim, and H. Levy II, The episodic nature of air pollution transport from Asia to North America, *J. Geophys. Res.*, *105*, 26,931–26,945, 2000.

Zhang, Y., K. R. Sperber, and J. S. Boyle, Climatology and interannual variation of the East Asian winter monsoon: Results from the 1979–95 NCEP/NCAR reanalysis, *Mon. Weather Rev.*, *125*, 2605–2619, 1997.

I. Bey and B. N. Duncan, Ecole Polytechnique Federale de Lausanne, CH-1015 Lausanne, Switzerland. (isabelle.bey@epfl.ch; bryan.duncan@epfl.ch)

D. J. Jacob and R. M. Yantosca, Department of Earth and Planetary Sciences and Division of Engineering and Applied Sciences, Harvard University, Cambridge, MA 02138, USA. (djj@io.harvard.edu; bmy@io.harvard.edu)

H. Liu, National Institute of Aerospace, 144 Research Drive, Hampton, VA 23666, USA. (hyl@post.harvard.edu)

G. W. Sachse, NASA Langley Research Center, Hampton, VA 23681-2199, USA. (g.w.sachse@larc.nasa.gov)

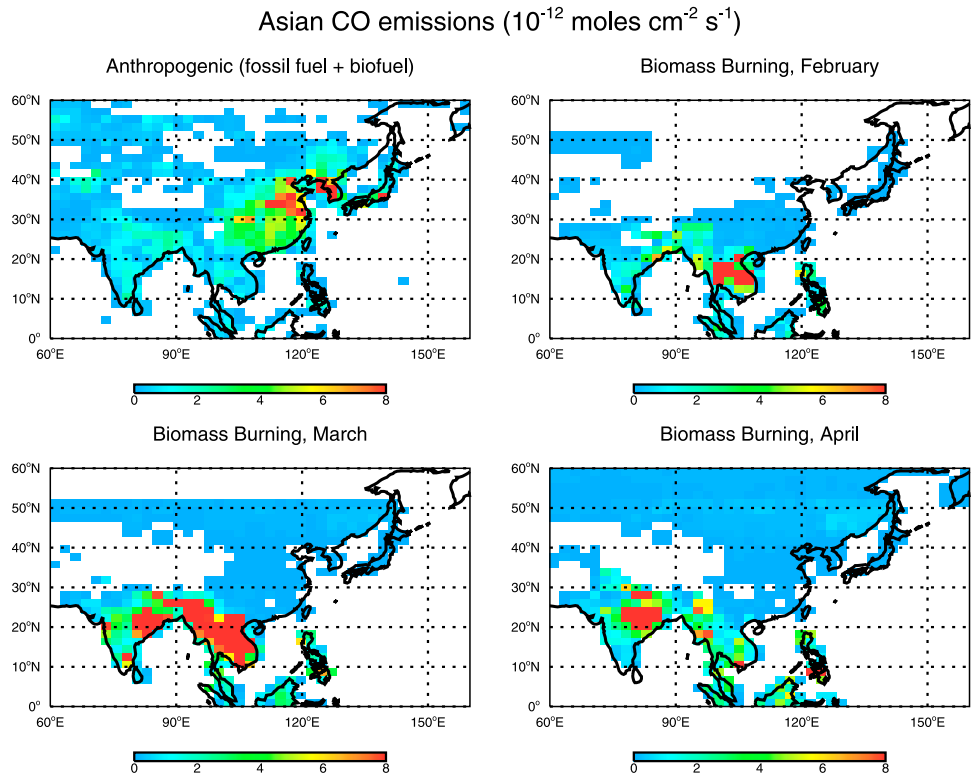

Figure 1. Asian CO emissions (10^{-12} moles cm^{-2} s^{-1}) used in the model for all simulation years.

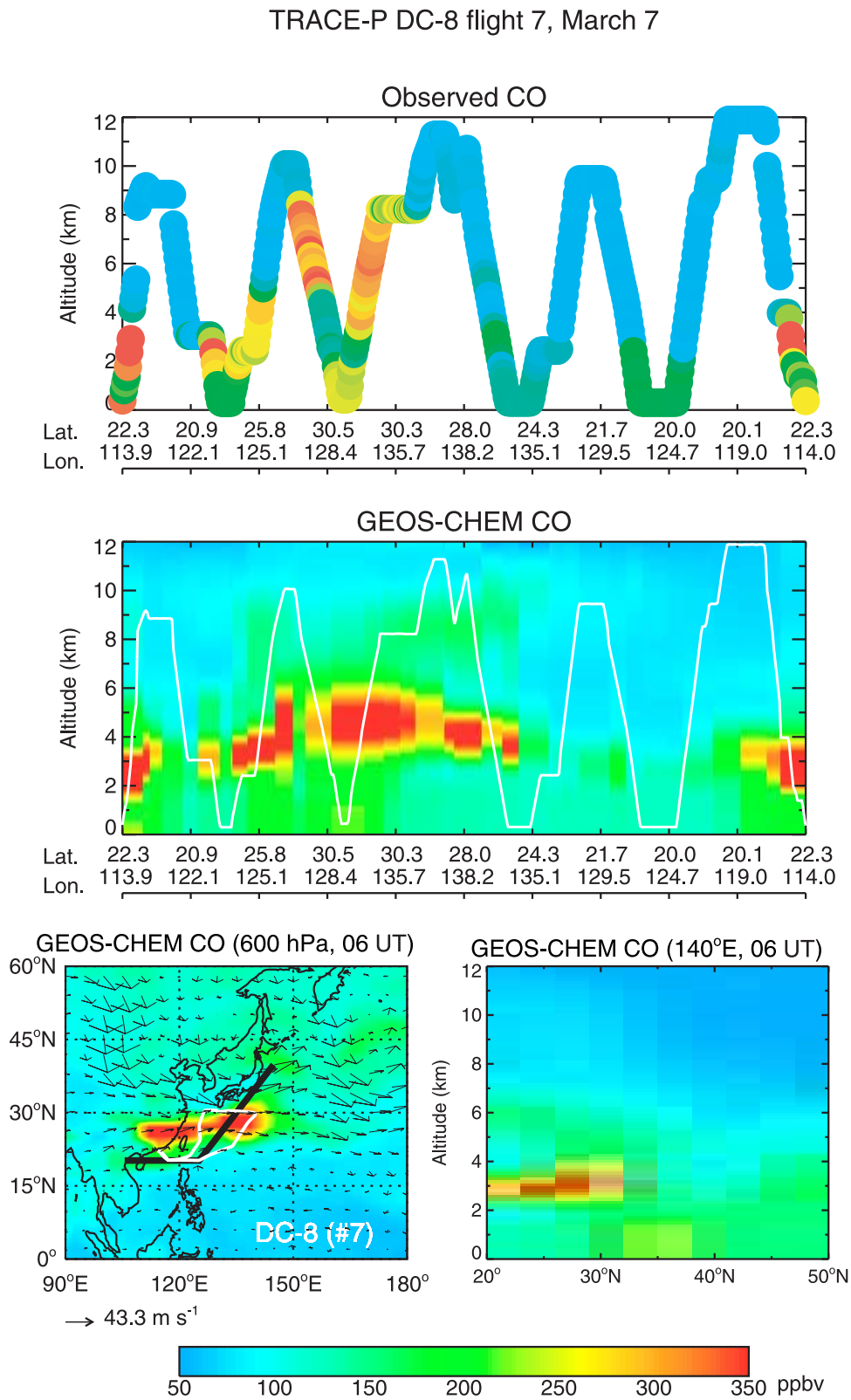

Figure 5. Frontal outflow in the lower free troposphere on 7 March 2001. DC-8 CO observations (top) are compared with model results (middle). The bottom left (map) shows the location of the surface cold front at 0600 UT (solid line), the DC-8 flight track (open line), wind vectors at 600 hPa, and simulated CO concentrations at 600 hPa. The bottom right shows the latitude-height cross section of the simulated CO at 140°E.

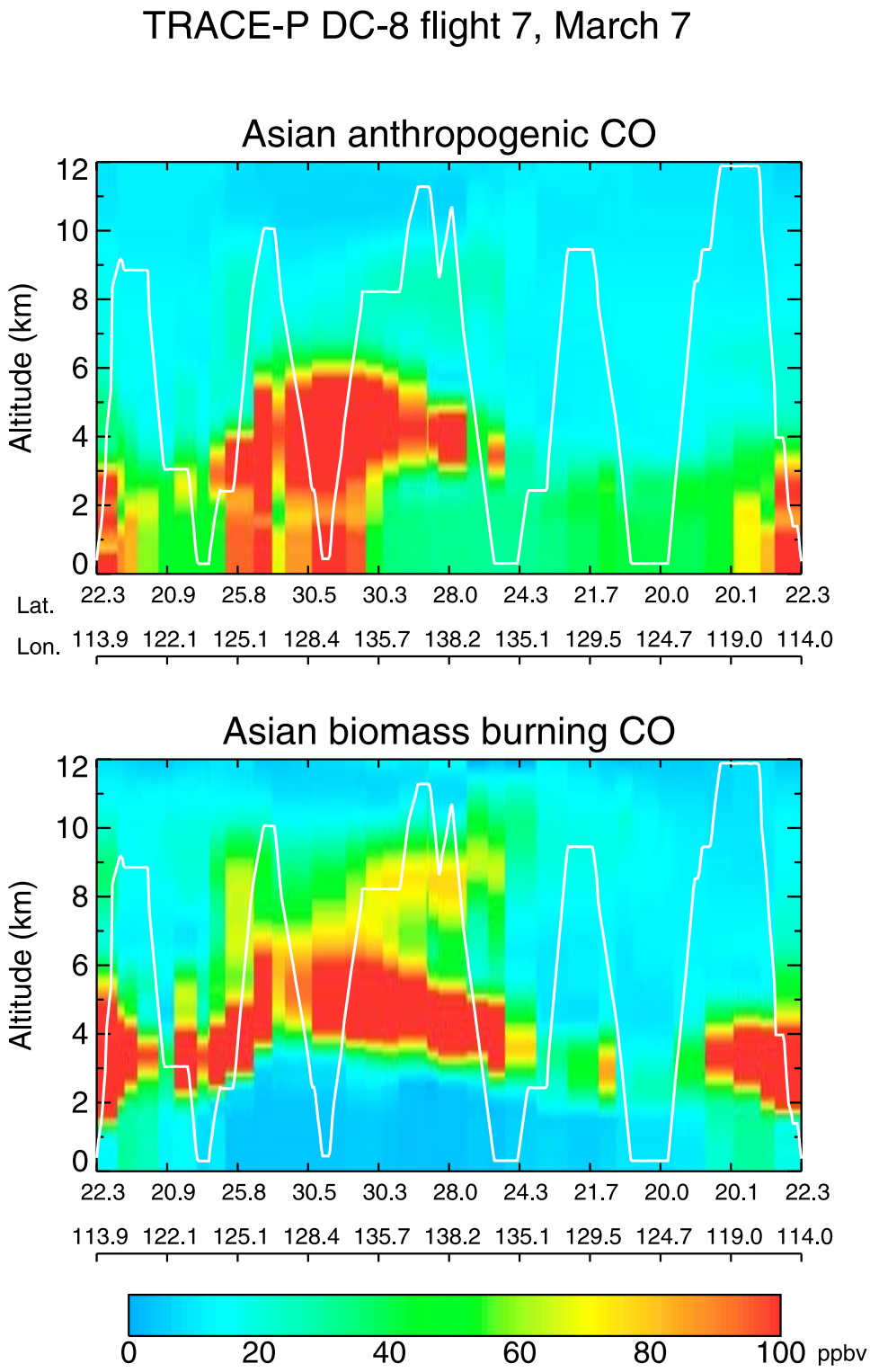

Figure 6. Simulated concentrations of Asian anthropogenic (top) and biomass burning (bottom) CO tracers along the DC-8 flight track (open line) on 7 March 2001.

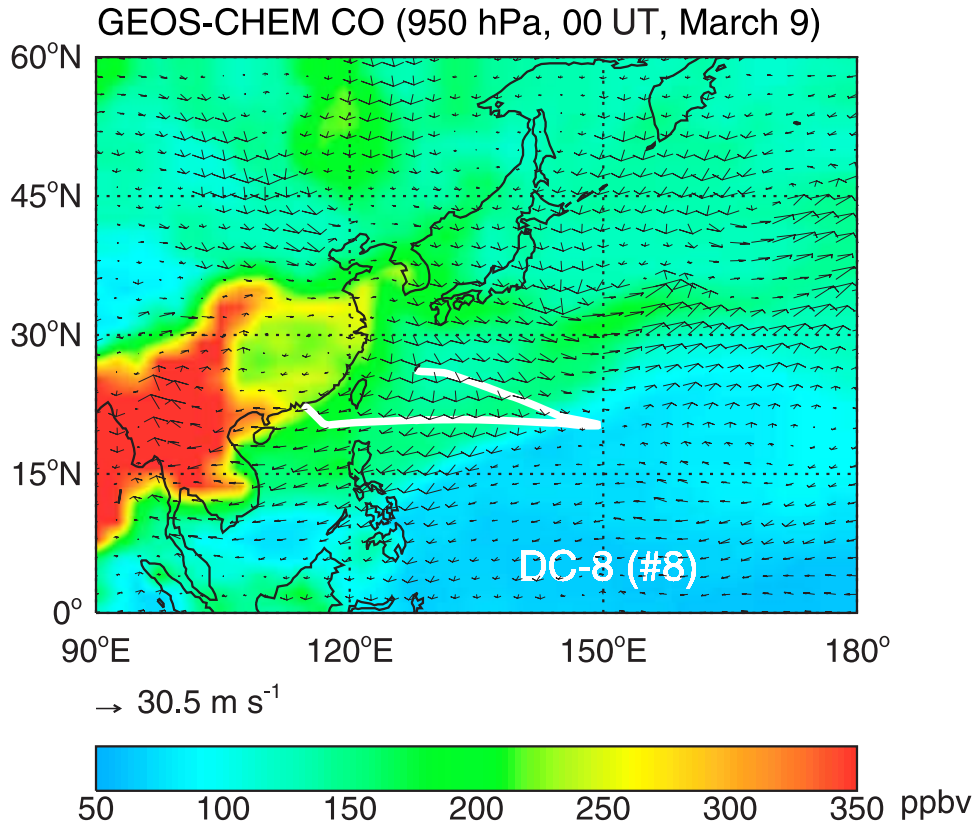

Figure 7. Simulated CO concentrations at 950 hPa on 9 March 2001, illustrating the boundary layer outflow of anthropogenic Asian pollution behind a cold front. Arrows are wind vectors, and the open line shows the DC-8 flight track.

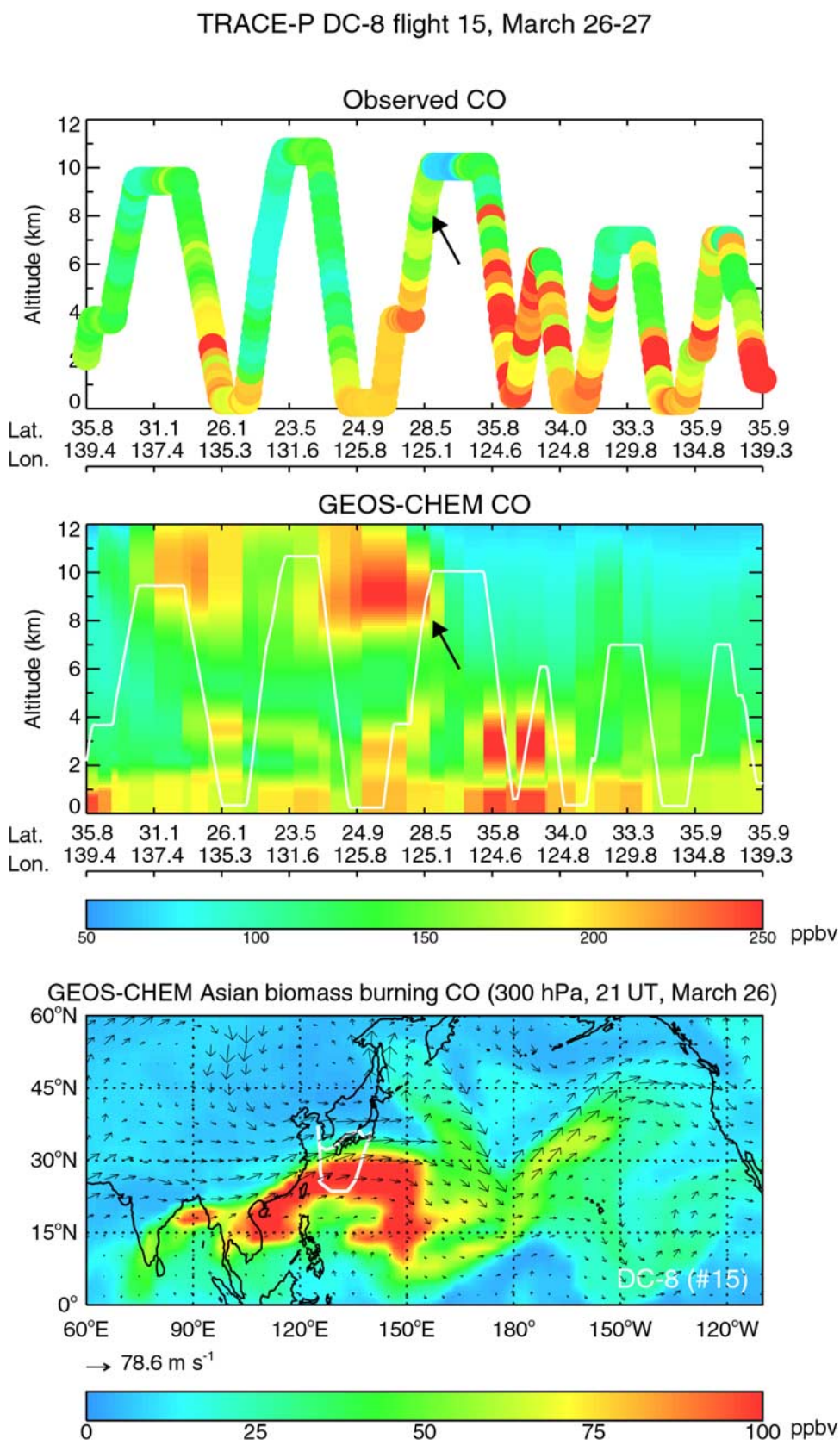

Figure 8. Convective outflow of Asian biomass burning CO in the upper troposphere on 26–27 March 2001. DC-8 CO observations (top) are compared with model results (middle). The bottom shows model Asian biomass burning CO concentrations at 300 hPa and 2100 UT, March 26. The open lines are the DC-8 flight track. Arrows in the top and middle indicate convective outflow. Arrows on the map are wind vectors.

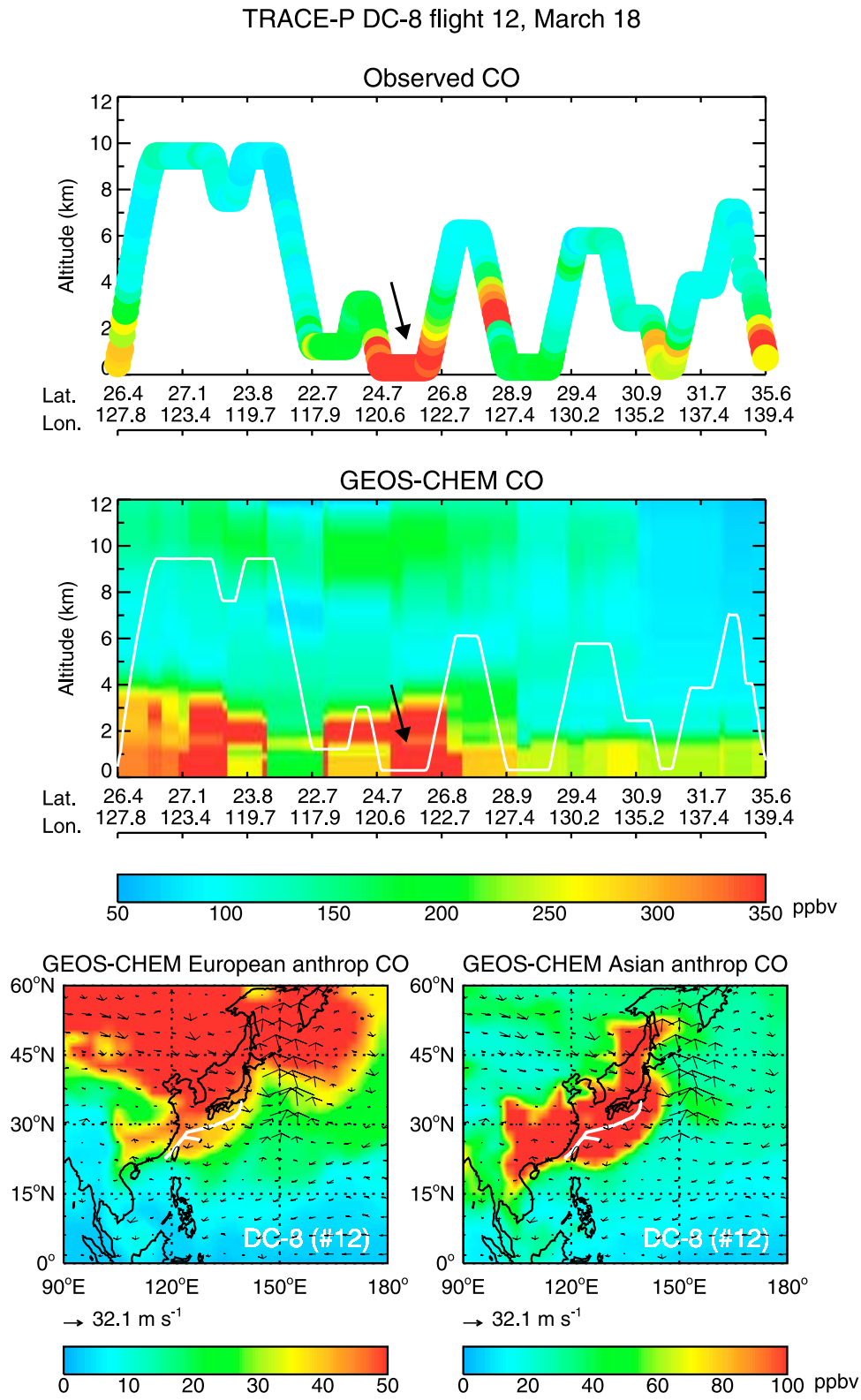

Figure 9. Postfrontal boundary layer outflow of Asian and European pollution on 18 March 2001. DC-8 CO observations (top) are compared with model results (middle) sampled along the DC-8 flight track (open line, bottom). The bottom shows the simulated concentrations of the European (bottom left) and Asian (bottom right) anthropogenic CO tracers at 950 hPa. Arrows in the top and middle indicate strong outflow in the boundary layer. Arrows on the map are wind vectors.

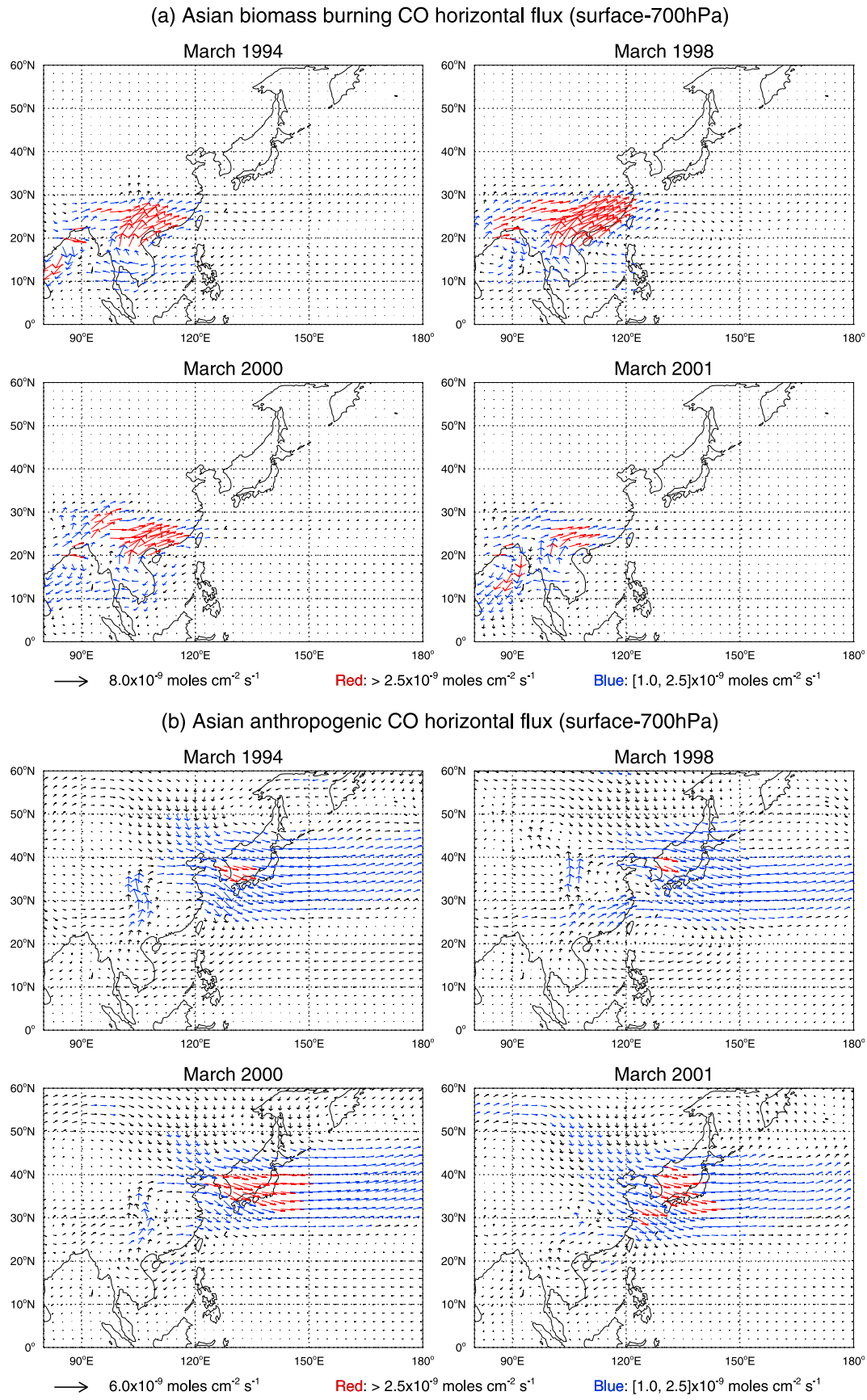

Figure 13. (a) Monthly mean horizontal fluxes of Asian biomass burning CO in March, shown for the 1000- to 700-hPa column and for 1994, 1998, 2000, and 2001, respectively. (b) Same as Figure 13a but for Asian anthropogenic CO.

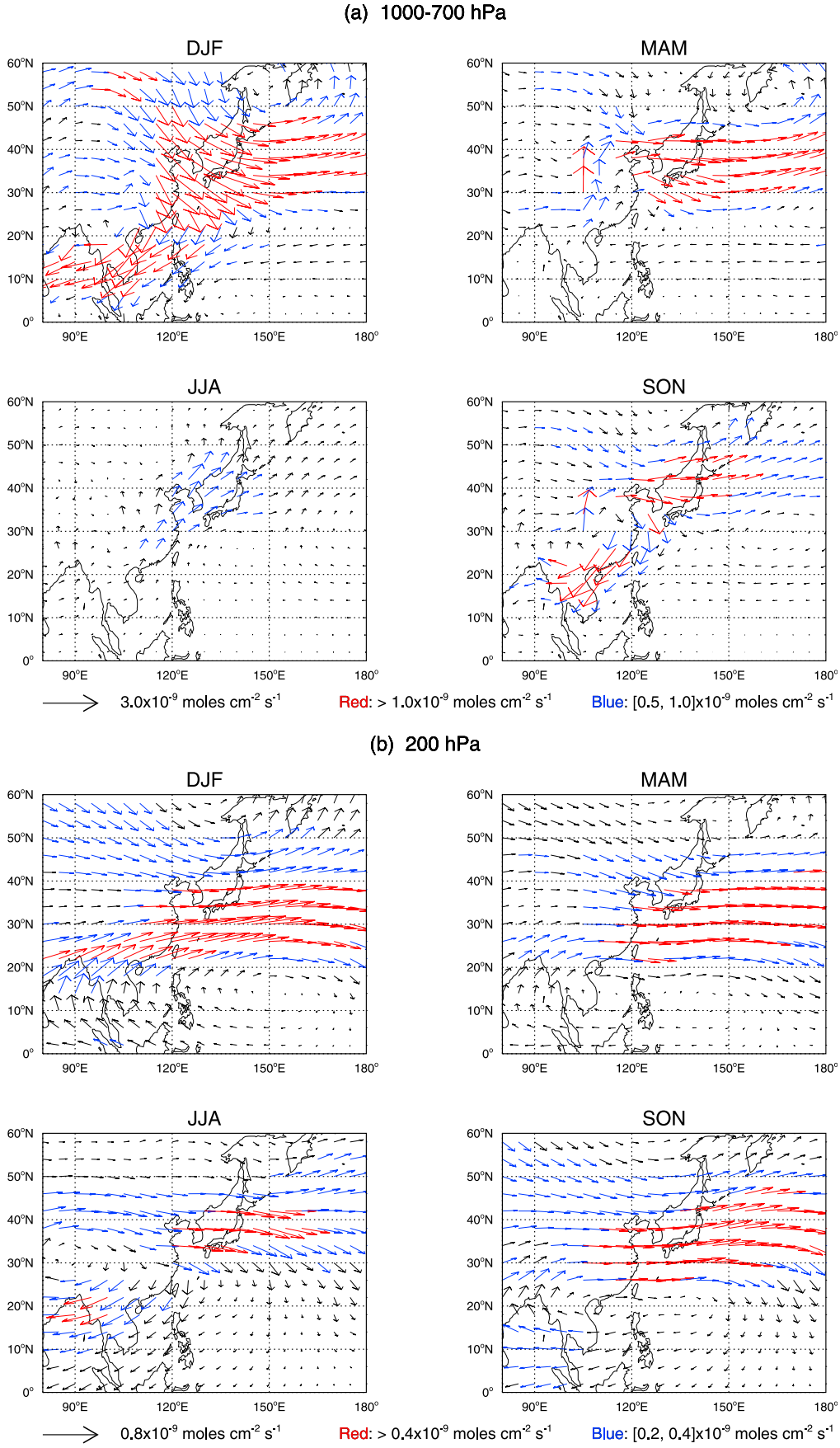

Figure 14. Horizontal fluxes of Asian anthropogenic CO, shown for (a) 1000- to 750-hPa column and (b) 200 hPa. Values are seasonal model averages for 1996.